

**Fermi National Accelerator Laboratory**

**FERMILAB-TM-2023**

# **KTeV Beam Systems Design Report**

V. Bocean et al.

*Fermi National Accelerator Laboratory  
P.O. Box 500, Batavia, Illinois 60510*

September 1997



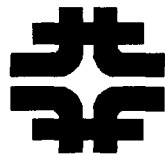
## **Disclaimer**

*This report was prepared as an account of work sponsored by an agency of the United States Government. Neither the United States Government nor any agency thereof, nor any of their employees, makes any warranty, express or implied, or assumes any legal liability or responsibility for the accuracy, completeness or usefulness of any information, apparatus, product or process disclosed, or represents that its use would not infringe privately owned rights. Reference herein to any specific commercial product, process or service by trade name, trademark, manufacturer or otherwise, does not necessarily constitute or imply its endorsement, recommendation or favoring by the United States Government or any agency thereof. The views and opinions of authors expressed herein do not necessarily state or reflect those of the United States Government or any agency thereof.*

## **Distribution**

*Approved for public release: further dissemination unlimited.*

# KTeV Beam Systems Design Report



Version 1.2  
September 1997

# KTeV Beam Systems Design Report

September 1997

V.Bocean, S.Childress, R.Coleman, R.Ford, W.Freeman,  
G.Gutierrez, D.Jensen, T.Kobilarcik, A.Malensek, D.Pushka,  
T.Sager, W.Slater, R.Tokarek, J.Wrbanek

We would like to thank the following people for many useful contributions, suggestions, and discussions:

M.Gerardi, Y.B.Hsiung, G.Thomson, J.Volk, H.White, B.Winstein  
L.Beverly, F.Browning, E.Chi, I.Churin, M.Crisler, R.Carrier,  
R.Fast, A.Lee, D.Mitchell, R.Nelson, F.Renken, G.Smith,  
R.Wands, G.Wocjik

Special thanks to:

Elaine Phillips and Laura Sedlacek

INTRODUCTION .....	1
1. OVERVIEW of KTeV BEAM SPECIFICATIONS.....	3
1.1 Intensity Parameters.....	3
1.2 Stability Requirements .....	4
1.3 Backgrounds.....	4
1.3.1 Charged Particles and Photons.....	4
1.3.2 Neutral Kaon and Lambda Decays.....	4
1.3.3 Neutral Beam (Kaons, Neutrons and a few Lambda's).....	4
1.4 Muon Rejection .....	5
1.5 KTeV Beam and Spectrometer System.....	5
1.5.1 Beam Elements.....	5
1.5.2 The Spectrometer.....	9
2. PRIMARY BEAM.....	12
2.1 Primary Beam Requirements.....	12
2.2 Magnets And Instrumentation Layout.....	13
2.2.1 Enclosure NM1.....	13
2.2.2 NM1 to NM2 Pipe.....	15
2.2.3 Enclosure NM2.....	16
2.3 The Angle Varying Bend (AVB) System.....	18
2.4 Optics .....	19
2.4.1 Goals .....	19
2.4.2 Constraints .....	20
2.4.3 Options.....	22
2.4.4 Design.....	25
2.5 Stability.....	31
2.5.1 Sources of Instabilities .....	31
2.5.2 Power Supply Stability.....	32
2.5.3 Canceling Slow Instabilities.....	33
2.5.4 SWIC Stability.....	38
2.5.5 Beam Roll.....	40
2.5.6 Conclusions.....	41
2.6 Target Scans.....	42
2.7 Instrumentation.....	42
2.7.1 NM1.....	42
2.7.2 NM2.....	43
2.8 Muon Halo.....	45

2.8.1	HALO Calculations and Impact.....	45
2.8.2	Operational Expectations, Control .....	48
2.9	Component Identification .....	48
2.10	RD/AD Beam Control Link.....	48
3.	CRITICAL DEVICES / INTERLOCKS.....	50
3.1	Primary Beam.....	50
3.1.1	Precluding Downstream Primary Transport .....	50
3.1.2	Critical Devices/Coupling with Neutrino Area .....	53
3.2	Secondary Beam.....	54
3.2.1	Critical Devices.....	54
3.2.2	Experimental Hall Interlocks .....	54
3.3	Access Issues.....	55
3.3.1	Access Requirements .....	55
3.3.2	Options Considered.....	55
4.	BEAM DUMP / MUON SWEEPING.....	58
4.1	Beam Dump System—Overview.....	58
4.1.1	System Function and Location .....	58
4.1.2	Component Function and Location .....	59
4.1.3	Apertures.....	62
4.2	Design and Installation.....	65
4.2.1	Target Sweeping Magnet—NM2S1.....	66
4.2.2	Primary Beam Dump—NM2BD .....	67
4.2.3	E8/Hyperon Magnet—NM2S2.....	68
4.2.4	Mu-sweep II—NM2S3 .....	69
4.2.5	Target Pile Shielding.....	70
4.2.6	Cooling.....	72
4.3	Installation .....	73
4.4	Muon Sweeping System.....	92
4.3.1	Design Criteria.....	92
4.3.2	Quality Assurance.....	93
4.3.3	System geometry .....	95
4.3.4	Rate projections.....	97
4.3.5	Conclusion .....	99
5.	SECONDARY BEAM .....	114
5.1	Secondary Beam Layout .....	114
5.2	Flux Calculations .....	115

5.3	Justifications for Beam Stability Requirements .....	118
5.4	Target Design .....	120
5.5	Primary Beam Dump Background Elimination.....	123
5.6	Elimination of Charged Particles from the Neutral Channel.....	125
5.7	Filter System—Photon Elimination and KL/n Enhancement.....	127
5.8	Collimator System.....	130
5.8.1	Design goals.....	130
5.8.2	System Layout.....	132
5.8.3	General Considerations of Collimator Outer Dimensions.....	134
5.8.4	Primary/Upstream Fixed Two-Hole Collimator .....	136
5.8.5	Defining/Downstream Fixed Two-hole Collimator.....	138
5.8.6	Alignment and Mechanical Tolerances.....	140
5.9	Beam Instrumentation/Monitoring .....	140
5.10	The Lambda Polarized Beam and Spin Rotations vs Sweepers .....	143
5.11	Secondary Beam Simulations of Radiation Damage/Backgrounds.....	144
5.11.1	Comparison of Data and Simulations with E731 and E799-I.....	144
5.11.2	Projections for KTeV—E799II and E832.....	162
6.	RADIATION SAFETY .....	173
6.1	Method.....	173
6.2	Beam Parameters .....	173
6.3	Primary Beam Line Shielding.....	174
6.4	Secondary Beam Line Shielding.....	175
6.5	Experiment Hall Shielding.....	175
6.5.1	Dose Rates and Shielding Requirements — Transverse Direction .....	176
6.5.2	Dose Rates and Shielding Requirements — Forward Direction .....	179
6.6	Neutron Skyshine.....	189
6.7	Labyrinths and Penetrations.....	190
6.8	Ground Water Protection .....	192
6.8.1	Description of Modeled Geometry.....	192
6.8.2	Method and Results .....	193
6.9	Residual Activation of Target Station.....	201

6.10	KAMI Operations.....	202
6.10.1	KAMI Primary Beam Shielding .....	203
6.10.2	"Decay Enclosure" (NM3) .....	203
6.10.3	KAMI Secondary Beam Shielding .....	203
6.10.4	KAMI Experiment Hall Shielding .....	204
6.10.5	Forward Shielding—KAMI.....	208
6.10.6	Labyrinths and Penetrations.....	208
7.	SITE AND UTILITY REQUIREMENTS .....	211
8.	INSTALLATION.....	215
9.	ALIGNMENT AND STABILITY.....	216
9.1.	Alignment and Stability Requirements.....	220
9.1.1	The Neutral Beam System.....	221
9.1.2	The Primary Beam.....	223
9.1.3	Detector Element Tolerances.....	224
9.2.	Methodology .....	236
9.2.1	External Survey Control Network.....	237
9.2.2	High Accuracy Internal Control Network.....	237
9.2.3	Network Preanalysis .....	239
9.2.4	Maintenance of the Internal Network and Monitoring of Relative Component Positioning .....	241
9.3.	Implementation.....	242
9.3.1	KTeV Civil Construction Issues.....	242
9.3.2	Stability.....	245
9.3.3	General Alignment and Fiducialization Procedures.....	252
9.3.4	Alignment Hardware Specifications .....	254
	APPENDIX 1.....	258
	APPENDIX 2.....	261

# KTeV Beam Systems Design Report

KTeV Beams Group  
Version 1.2 September 1997

## Abstract

The primary and secondary beams for the KTeV experiments E799-II and E832 are discussed. The specifications are presented and justified. The technical details of the implementation of the primary beam transport and stability are detailed. The target, beam dump, and radiation safety issues are discussed. The details of the collimation system for the pair of secondary beams are presented.

## INTRODUCTION

In this document, we present a discussion of the beams for the KTeV experiments: E799-II and E832 <sup>1,2</sup>. The primary and secondary beam specifications are closely related and are therefore discussed together.

Experiment E799-II is a study of rare  $K_L$  decays where the decays take place in approximately 60 meters of vacuum decay pipe. Experiment E832 is a measurement of  $e'/e$  in the neutral K system. A thick regenerator, located in the vacuum decay region, will be moved spill-by-spill between the two neutral beams to produce  $K_S$ 's. The kaon decay products are detected, identified and measured using the charged particle detection system and the CsI calorimeter that comprise the detector system.

---

<sup>1</sup> Fermi Lab Proposal E799.

<sup>2</sup> Fermi Lab Proposal E832.

A general feature of the beam system is a primary proton beam impinging on one interaction length of BeO to produce a pair of "identical" neutral beams side by side. The beams are rendered neutral by a set of sweeping magnets and collimators. A system of magnetic sweeping and shielding is designed to reduce the muon flux from both the target and beam dump sources. There is careful monitoring of the size, direction and intensity of the primary beam. The unspent primary must be dumped in such a manner as to not create excessive backgrounds. The secondary beam has five collimators: two of these are fixed-hole collimators (referred to as primary and defining collimators in this report); one is a slab collimator designed to prevent particles from scattering out of one beam (in the plan view) into the adjacent beam and hitting the calorimeter; and two are variable jaw collimators used to reduce the flux on the defining collimator if needed. The neutral beam must pass cleanly through the holes in the CsI.

The report is divided into 9 sections listed below:

1. Overview of KTeV beam specifications
2. Primary beam
3. Critical devices/interlocks
4. Beam dump/muon sweeping
5. Secondary beam
6. Radiation safety
7. Site and utility requirements
8. Installation
9. Alignment and long term stability

Where appropriate, other documents are cited and the results noted are only very briefly summarized in this document.

# 1. OVERVIEW of KTeV BEAM SPECIFICATIONS

## 1.1 Intensity Parameters

A primary beam intensity of  $5 \times 10^{12}$  ( $3.5 \times 10^{12}$ ) protons per Tevatron cycle yields acceptable rates consistent with the proposal.<sup>3,4</sup> The  $K_L$  fluxes are calculated using the Malensek parameterization<sup>5</sup> normalized to measured  $K_L$  decay rates measured in E731.<sup>6</sup> These fluxes are discussed in more detail in the secondary beam section.

## 1.2 Stability Requirements

It is necessary, for experiment E832, that the sizes and positions of the two neutral beams be stable to 0.5 mm, that the areas be equal (to 1%), and that the kaon momentum spectra be equal (to 0.1%).<sup>7</sup> These conditions must be maintained during each spill and for the duration of the experiment, and also imply certain stability requirements on the primary beam, target, and collimators. Experience, particularly during E731, demonstrates that it is an important issue. The requirements on the primary beam are:

1. beam size on targets < 0.25 mm in x and y
2. beam size stability 10%
3. beam positional stability  $\pm 0.1$  mm
4. angular stability  $\pm 25$   $\mu$ rad

These requirements and how they were derived are discussed in section 5.3.

---

<sup>3</sup> Fermi Lab Proposal E799.

<sup>4</sup> Fermi Lab Proposal E832.

<sup>5</sup> A. J. Malensek, Fermi Lab FN-341.

<sup>6</sup> J.R. Patterson, "Determination of  $\text{Re } \epsilon'/\epsilon$  by the Simultaneous Detection of the Four  $K_{LS} \rightarrow \pi\pi$  Decay Modes", Dec. 1990, U. Chicago dissertation.

<sup>7</sup> D. Jensen, "On the Sensitivity of  $\epsilon'/\epsilon$  to Primary Beam Parameters", Feb. 2, 1994, KTeV memo.

## 1.3 Backgrounds

### 1.3.1 Charged Particles and Photons

The magnetic sweeping of charged particles from the primary target must be sufficient to remove any noticeable effect from these charged particles relative to the number of charged particles from decays. In addition, copiously produced photons from the target must be removed by placing a lead filter in the beam.

### 1.3.2 Neutral Kaon and Lambda Decays

Our goal is to keep background rates from the neutral beam comparable to the detector rate and trigger rate from neutral kaon decays. For example, the rate of single muons from  $K_{\mu 3}$  decays occur at the rate of 20 (120) kHz for E832 (E799-II) at the CsI. The rate from lambda decays is about 10% of the rate of kaon decays in the detector.

### 1.3.3 Neutral Beam (Kaons, Neutrons and a few Lambda's)

#### Interactions with Material in the Beam Path

Filters to reduce the photon and neutron products in the beam introduce a source of elastic and inelastic interactions.

In E832 the regenerator (100 cm of scintillator) is a significant source of background as well as trigger hodoscope (2 cm of scintillator) for both experiments.

#### Interactions with Collimator/Magnet Apertures

Additional neutral beam background arises from the interaction of target spray and decay products which strike the inner walls of the neutral channel. In addition the filters introduce additional scattering of the beam which again strikes the neutral channel walls or could leave the "beam hole" and strike the electromagnetic detector.

In previous experiments, radiation damage to the electromagnetic calorimeter near the neutral beam holes was a significant problem. A discussion of radiation damage and backgrounds are summarized in section 5.8. While KTeV is running at higher proton intensity (approximately three times higher), CsI is less sensitive to radiation damage than the previous Pb glass calorimeter.

## **1.4 Muon Rejection**

The goal is to reduce the muon halo rate in the spectrometer from primary target and beam dump sources to 100 kHz at  $5 \times 10^{12}$  incident protons per spill. This is comparable to the projected inherent muon rate from  $K_{\mu 3}$  decays of 20 (120) kHz for E832 (E799II) at the CsI, of which about 1/4 remain in the beam channel. The radiation dosage at the experimental counting room should also be well within specified personnel safety levels, as should outdoor area muon rates.

## **1.5 KTeV Beam and Spectrometer System**

The general description of the beam and spectrometer systems for KTeV is presented in this section. The KTeV primary beam follows the same initial trajectory to Enclosure NM1 as the previous NMUON beam line, and uses existing enclosures for primary beam transport and targeting. A pair of neutral beams, as defined by appropriate collimation, emerge into a large evacuated decay volume. This region is surrounded by an annular photon veto system. Decay products exit through a thin vacuum window to a detection apparatus consisting of a calorimeter, tracking and magnetic spectrometer, veto counters and particle identification systems. More detailed discussions of each system are presented below.

### **1.5.1 Beam Elements**

A plan view layout of the beam system is given in Figure 1.5.1. Shown in this figure are the relative location of components and their respective sizes. The KTeV primary beam follows the transport from the Tevatron along the current Switchyard muon beam line. Existing dipoles in the upstream NM1 enclosure are utilized to raise the entrance beam height into enclosure

NM2. The upstream section of the existing NM2 enclosure is utilized for the pretarget beam elements. These elements include a pair of B2 dipoles for establishing the final beam trajectory, final focus quadrupoles, AVB dipole string for control of the beam targeting angle, and instrumentation for beam position and intensity measurement.

The primary target, beam dump, muon sweeping magnets, initial neutral secondary beam collimation, and beam filters are positioned in the existing NM2 target hall.

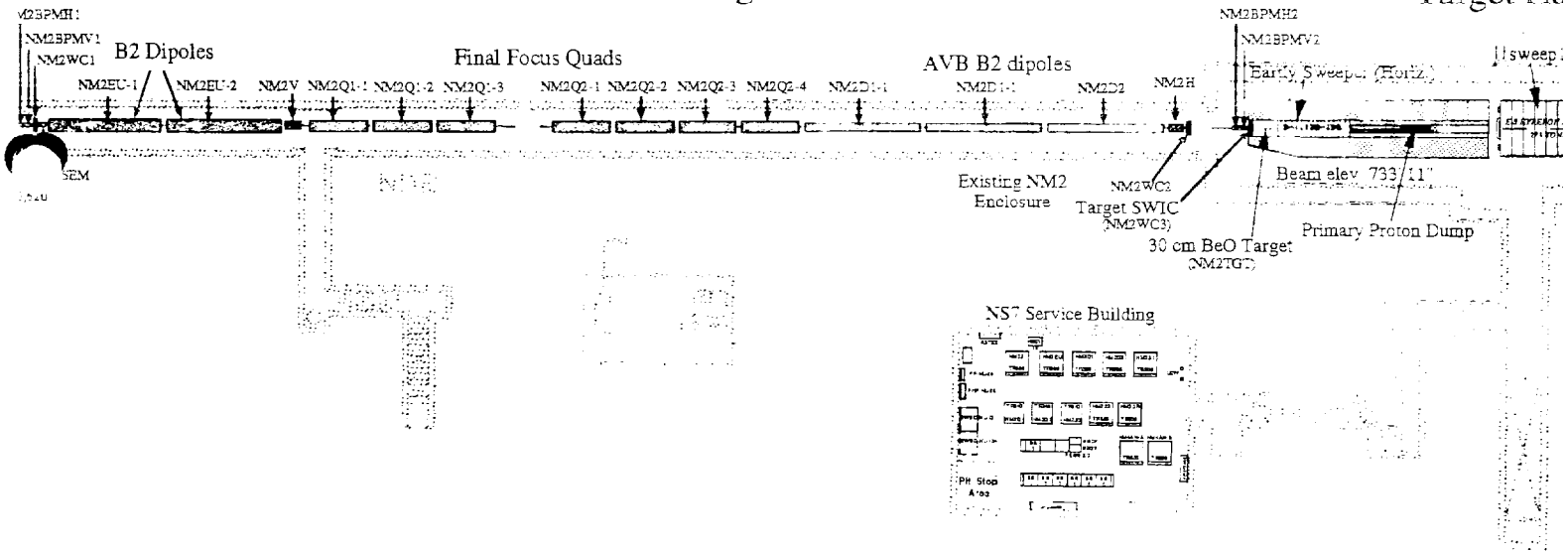
Subsequent secondary beam elements are located in the downstream section of the existing NM2 enclosure, and in a new upstream extension to the existing NM3 enclosure. The function of these elements is to provide definition of the two horizontally separated kaon beams and to provide cleanup of charged and neutral particle backgrounds. It is important to note that since the beam can no longer be steered with magnets that the only control over the size, direction, and symmetry of the two beams is by collimation. This is the main reason alignment and stability play such an important role in the experiment. Beam transport between enclosures NM2 and NM3 is through a buried beam pipe as shown in the figure. Also shown is an offset alignment sight pipe which is used for referencing precision collimation elements between the two enclosures.

# KTeV Beamline



Pre-target Area

Target Hall



# Layout

Rev. 1  
Version 3.0  
2/6/94

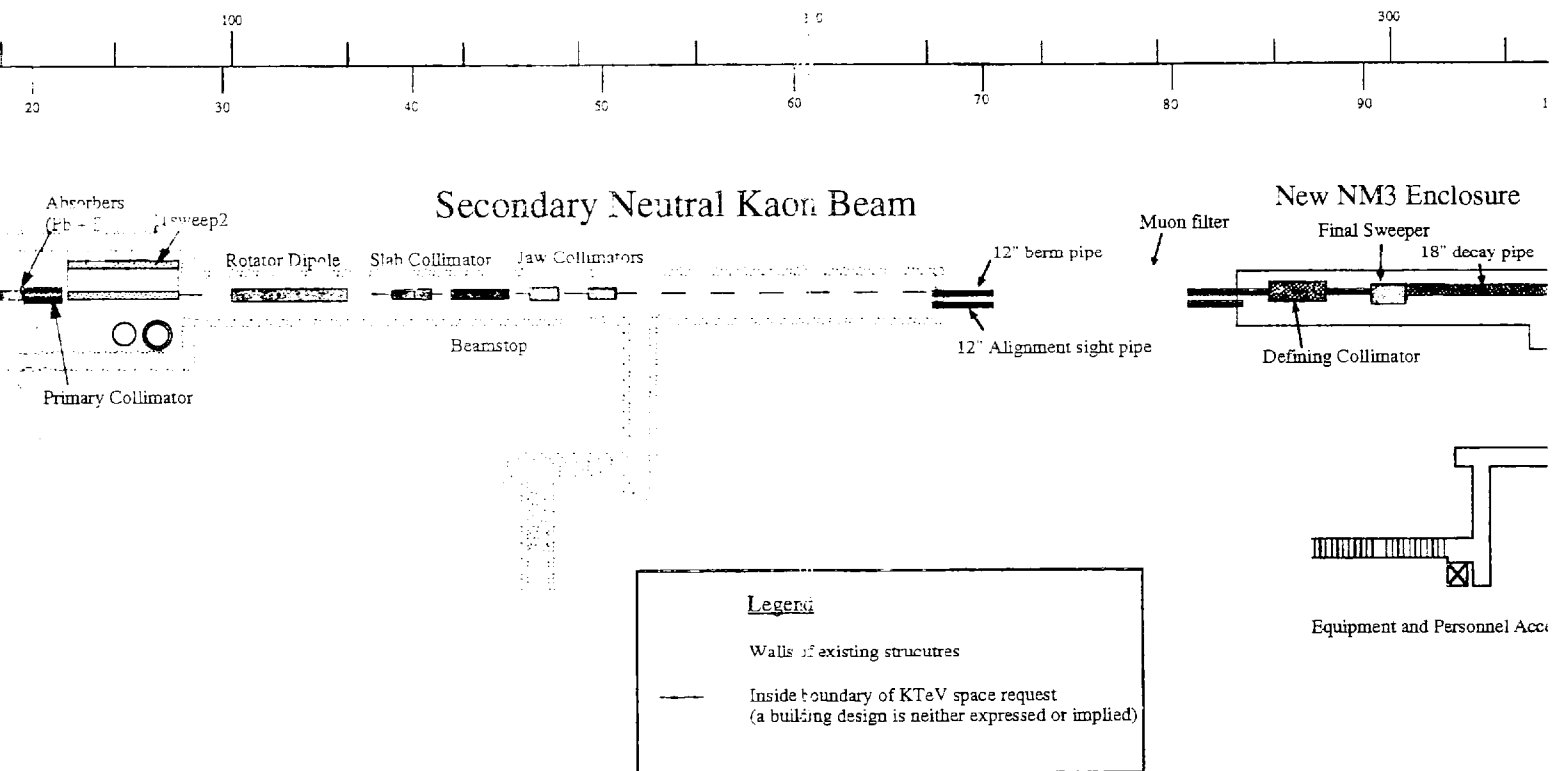


FIGURE 1.5.1

## 1.5.2 The Spectrometer

A kaon decay region begins downstream of the final secondary beam collimation element and final sweeping magnet. The decay region opens into successively larger diameter pipes. For the rare decay experiment E799, the decay region begins at the 20 inch diameter pipe in the new NM3 extension, immediately downstream of the defining collimator and final sweeper magnet. This region provides a vacuum channel for particle decays and the neutral beam transport to the decay building and experimental hall. For E832, the decay region begins after a mask anti and active regenerator, elements which are removed for the E799 experiment. To house these components and the downstream decay region with instrumented veto ring counters, a new decay enclosure is required. This decay enclosure is located between NM3 and the new KTeV experimental hall.

The regenerator sits in vacuum and is moved to alternate beam positions between each beam spill. Its function is to provide a  $K_S$  beam from the incident  $K_L$  beams. This device is followed by a series of large vacuum vessels ranging in diameter from 200 cm to 240 cm. The vessels are connected together between successive ring veto counters to form a continuous vacuum region. The ring veto counters, labeled RC6-RC10, are designed to catch wide angle photons from background  $3\pi^0$  decays and to eliminate other background events for rare decay modes. A 1.8 meter diameter thin window of Kevlar and aluminized Mylar terminates the vacuum volume.

The detector consists of drift chambers, veto counters, analysis magnet, transition radiation detectors, electromagnetic calorimeter, triggering hodoscope, and muon detection system. The four sets of drift chambers (labeled DC1-DC4), were used in the last experiment and are now being refurbished for KTeV. These chambers have resolutions of less than 100 microns. Each chamber has two horizontal planes ( $x$  and  $x'$ ) and two vertical planes ( $y$  and  $y'$ ). These existing chambers will be used with fast chamber gas and new pre-amplifiers. The most upstream drift chamber, DC1, is placed at the end of the vacuum decay region. The other three chambers are supported by the spectrometer anti stands. Bags of helium gas are placed along the beam

line downstream of the vacuum region to reduce the scattering of secondary particles in the spectrometer. The four sets of drift chambers and the analyzing magnet will be used to measure the momenta and the decay vertex of the charged particles from kaon decays.

The "Spectrometer Anti" (SA) veto counters are lead and scintillator sandwich modules, rectangular in shape, which are used to detect and veto all particles within their active areas. There are four of these counters, including three (SA2-SA4) associated with a concordant numbered drift chamber and one (CIA) located near the CsI calorimeter. Each of these pairs will have a rigid aluminum and steel stand, supporting both a drift chamber and a veto module. They are located approximately equally spaced (relative to the magnet) after the decay region and before the calorimeter.

The SA, CIA and RC counters, together with the CsI and BA (see below) form a hermetic detector. All decay products with angles out to approximately 100 mrad with respect to the beam direction are detected with high efficiency.

The KTeV spectrometer magnet, in conjunction with the drift chambers, is used to measure the momenta of the charged particles from kaon decays. This magnet weighs 206 tons, with a 2.03 meters vertical by 2.90 meters horizontal gap. This device uses aluminum coils and, at a transverse momentum kick of 450 MeV/c, consumes approximately 400 kilowatts of power. The magnet is located between the SA2 and SA3 counters.

With a field integral of 400 MeV/c, for example, the momentum resolution is better than one percent up to 50 GeV/c, decreasing to 3 percent at 250 GeV/c.

Particle identification is achieved in part by using transition radiation detectors (TRD's). TRD1-TRD10 will be used to distinguish between pions and electrons. These detectors are located downstream of the last drift chamber. A scintillation trigger hodoscope system will also be placed in this region and used to form a fast trigger for charged particles.

The Cesium Iodide (CsI) array is the crucial detector for the KTeV experiments. It is located 1.5 meters downstream of the trigger hodoscope. This precision high-resolution electromagnetic (EM) calorimeter is the sole detector for reconstructing neutral mode kaon decays. This is accomplished by measuring the energy and position of photons from  $\pi^0$  decays. The calorimeter consists of an array of 50 cm long blocks of pure CsI. Transverse dimensions of the array are 1.9 meters by 1.9 meters, with a total of 3100 CsI blocks. This electromagnetic calorimeter will have an energy resolution of better than one percent and a position resolution of order 1 mm.

There will be two 15 cm square beam holes horizontally separated by 30 cm. center to center in the CsI calorimeter array for the neutral beams to pass through. Another instrumented defining aperture (the "Collar Anti") is located just upstream of the CsI calorimeter beam holes, and partially covers the CsI blocks surrounding the beam holes. The Collar Anti will also provide a well defined aperture for acceptance calculations.

Downstream of the calorimeter, a scintillator hodoscope behind a lead wall will serve as a hadron veto for purely electromagnetic decay triggers. There will be a beam hole in the hadron veto, and lead wall for the two beams to pass through. There will be a Beam TRD (bTRD) in the neutral beam to distinguish pions from protons (in hyperon decays) in the neutral beam downstream of the CsI. A beam hole veto calorimeter ("Back Anti") will be placed after the lead wall to tag forward decay photons and electrons that escape the calorimeter down the beam hole. A lead and scintillator stack will be used for the front electromagnetic section, and an iron scintillator stack will be used for the hadronic section.

The muon detection and veto systems downstream of the beam hole veto system consist of an iron muon filter instrumented with scintillator hodoscope planes. The purpose of the muon system will be to veto particle signals in particular decays, and serve as a muon identifier to reduce backgrounds in other decays. The muon filter also serves as the neutral beam dump.

## 2. PRIMARY BEAM

### 2.1 Primary Beam Requirements

The specifications for the primary proton beam are summarized in Table 2.1.1.

Table 2.1.1  
Primary Beam Specifications

Proton beam energy	800/900 GeV
Proton intensity	$5 \times 10^{12}$ protons per spill
Targeting angle	-4.8 mr (vertical) 0.0 mr (horizontal)
Targeting angle variability	-4.0 mr to -5.6 mr (vertical)
Beam size at the target ( $\sigma$ )	$\leq 250 \mu\text{m}$ (horizontal and vertical)
Beam position stability	$\leq \pm 100 \mu\text{m}$ (horizontal and vertical)
Beam angle stability	$\leq \pm 25 \mu\text{rad}$ (horizontal and vertical)

Once the beam size at the target has been chosen the minimum beam divergence is given by the emittance. The emittance cannot be decreased after extraction because it is defined by the accelerator. The emittance values obtained by C.D. Moore et al.<sup>8</sup> will be used:  $\epsilon_{\text{H}} = 8\pi \text{ mm } \mu\text{rad}$  horizontally, and  $\epsilon_{\text{V}} = 6\pi \text{ mm } \mu\text{rad}$  vertically. The emittance is defined here as  $\epsilon = \sigma_x \sigma_y \pi \text{ mm } \mu\text{rad}$ .

With a horizontal beam waist at the target, a beam size of about  $\sigma_x = 150 \mu\text{m}$  is expected. Using the above emittance a horizontal beam divergence of  $\sigma_{\theta} = 60 \mu\text{rad}$  is expected. Similar numbers are expected for the vertical beam size and divergence.

---

<sup>8</sup> "Tevatron Extraction Model," by C.D. Moore, R. Coleman, G. Goderre, M. Yang.

## 2.2 Magnets And Instrumentation Layout

For the KTeV beam line only modifications in enclosures NM1 and NM2 are needed. The modifications in enclosure NM1 are minor. The next fixed target run is expected to be at an energy of 800 GeV. The designed KTeV primary beam line will be able to run up to 900 GeV.

### 2.2.1 Enclosure NM1

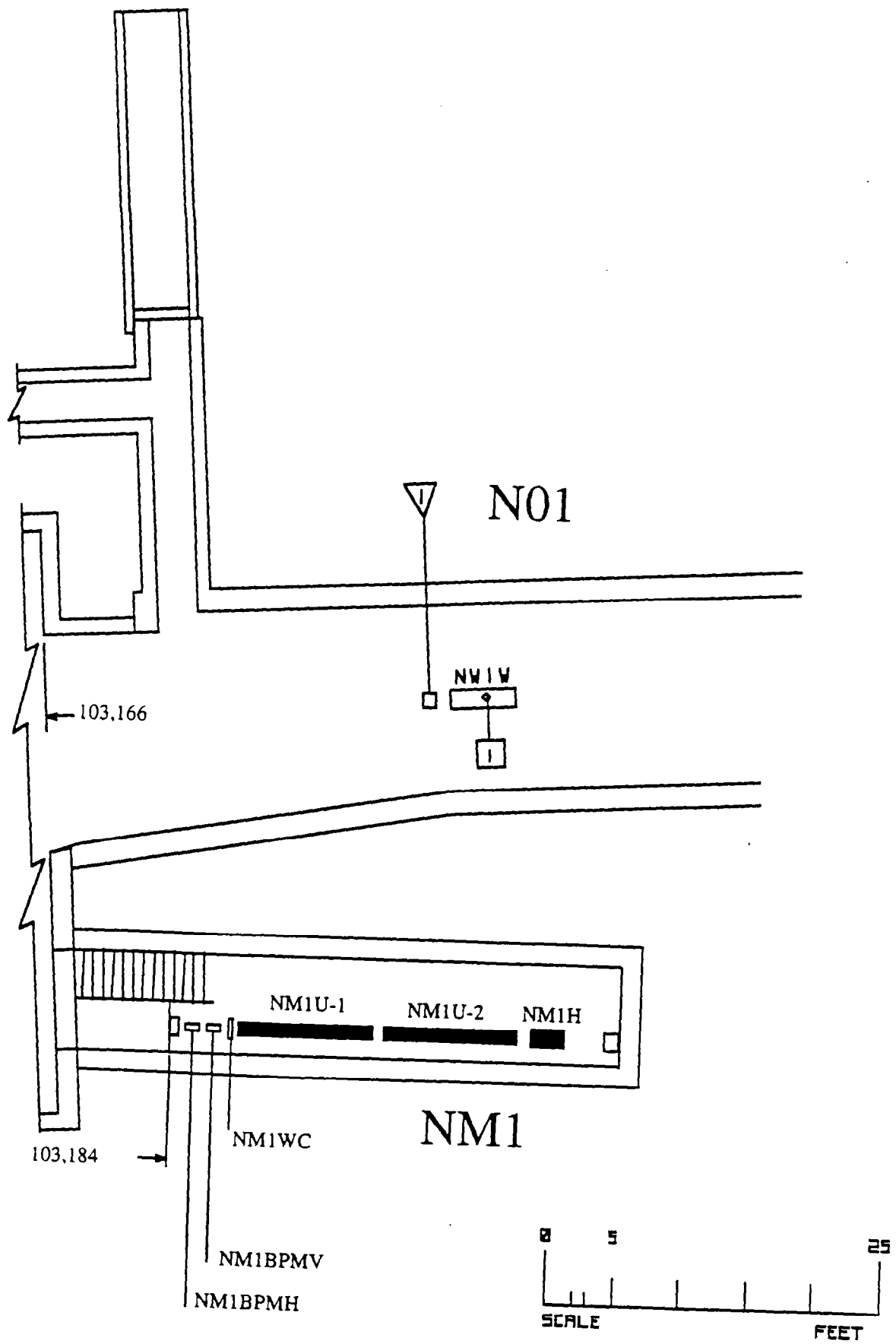
Figure 2.2.1 shows the magnet and instrumentation layout in enclosure NM1. There are two EPB magnets (NM1U), a trim magnet (NM1H), two short BPMs (NM1BPH and NM1BPV), and a vacuum SWIC (NM1WC). These elements essentially fill all the available space.

The NM1U EPBs will be running at higher currents than in previous runs. This will be done to raise the beam at the KTeV target in order to meet the Ground Water Activation limits (in the Single Resident Well model). NM1U will bend up 3.433 mr. At 800 GeV/c this can be done with two EPBs running at 1660 amps. At 900 GeV/c the two EPBs would have to run at 2125 amps<sup>9</sup>.

The BPMs and the vacuum SWIC will allow us to run with no material in the beam. Monte Carlo studies show that this is necessary in order to minimize the muon flux in the detector due to beam halo (see section 2.8).

---

<sup>9</sup> Leon Beverly indicates that this is viable current with ramped EPBs. The EPBs could be replaced by a B2 for 900 GeV if reliability problems occur.



Beamline component layout of NM1  
 FIGURE 2.2.1.

### 2.2.2 NM1 to NM2 Pipe

In order to raise the primary target as much as possible, the primary beam was placed two inches from the top of the NM1 to NM2 pipe. To see how much the beam could be raised, the pipe was surveyed. Figure 2.2.2 shows the results of the survey of the NM1 to NM2 pipe. This survey was done measuring the elevation of a target that was pulled from one end of the pipe to the other. In this way the bottom of the pipe was measured; the top was calculated using the pipe diameter (16 inches upstream, 24 inches downstream). The elevation of the low point on the top of the pipe was then verified by looking with an optical instrument from NM2 to NM1. The closest vertical point between the KTeV beam and the pipe is two inches. Horizontally the beam is centered in the pipe.

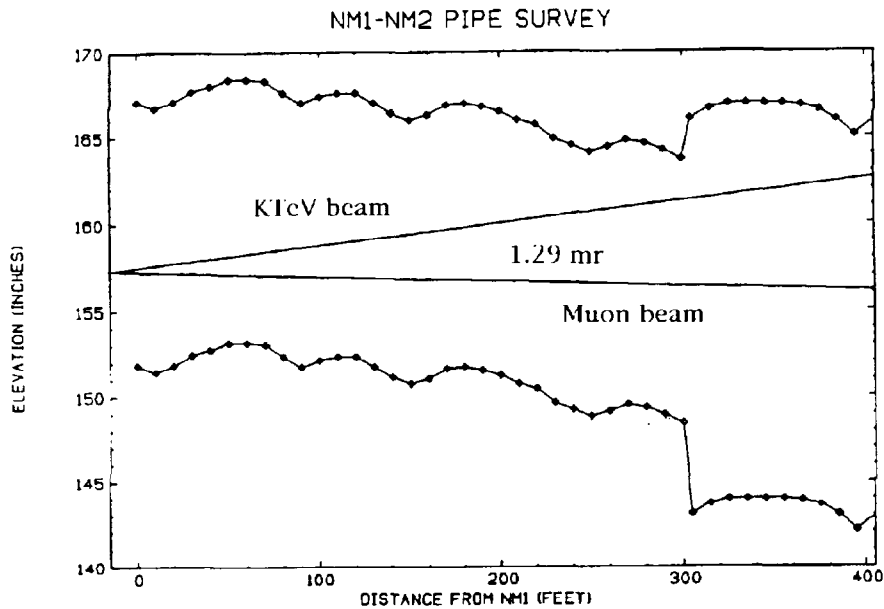


Figure 2.2.2  
NM1 to NM2 pipe survey. The pipe is 450 ft. long.  
Also shown are the NM beamline (labeled "Muon beam") for past runs and  
the new KTeV beam.

### 2.2.3 Enclosure NM2

Figure 2.2.3 shows the magnet layout in enclosure NM2. Three conflicting issues have to be resolved: a) to increase the target height, the up bend in NM2 should be as far upstream as possible and the down bend as far downstream as feasible (also needed is an east bend to match the existing enclosure downstream of the target), b) to increase the accuracy of beam position and slope measurement, one position measuring device should be very close to the target and another one as far upstream as possible, and c) to maximize its range, the Angle Varying Bend (AVB) system needs to be close to the target. The conflict is resolved as follows.

At the upstream end, after leaving about 6 feet for instrumentation, the beam is bent east and up by NM2EU, a string of two B2s is rotated 30.4 degrees. A vertical trim (NM2V) follows NM2EU, allowing for independent adjustment in the horizontal and vertical planes. At the downstream end, one position measuring device (NM2WC3) is located two feet upstream of the target, and a second (NM2WC2) about 10 feet upstream of the previous one—this allows extrapolation to the target with minimal loss in position resolution. The AVB system (NM2D1/NM2D2) is placed upstream of NM2WC2 (the horizontal trim NM2H is inserted here for fine control). The final focusing quadrupoles (NM2Q1/NM2Q2) are placed in the remaining space, between NM2EU and the AVB system. The KTeV target is eleven inches higher than the previous muon target. This gain in elevation was achieved by positioning the beam two inches away from the top of the NM1 to NM2 pipe and by bending the beam up with NM2EU and back down with NM2D1 and NM2D2. If needed, the beam may be repositioned without changing the target position, although this would reduce the range of the AVB system<sup>10</sup>.

---

<sup>10</sup> At 900 GeV/c, the beam can be lowered at the upstream end of NM2 by 2.6 inches by reducing the range of the AVB system from -4.0 to -5.6 mr to -4.0 to -4.8 mr. This will put the beam 4.6 inches away from the top of the pipe.

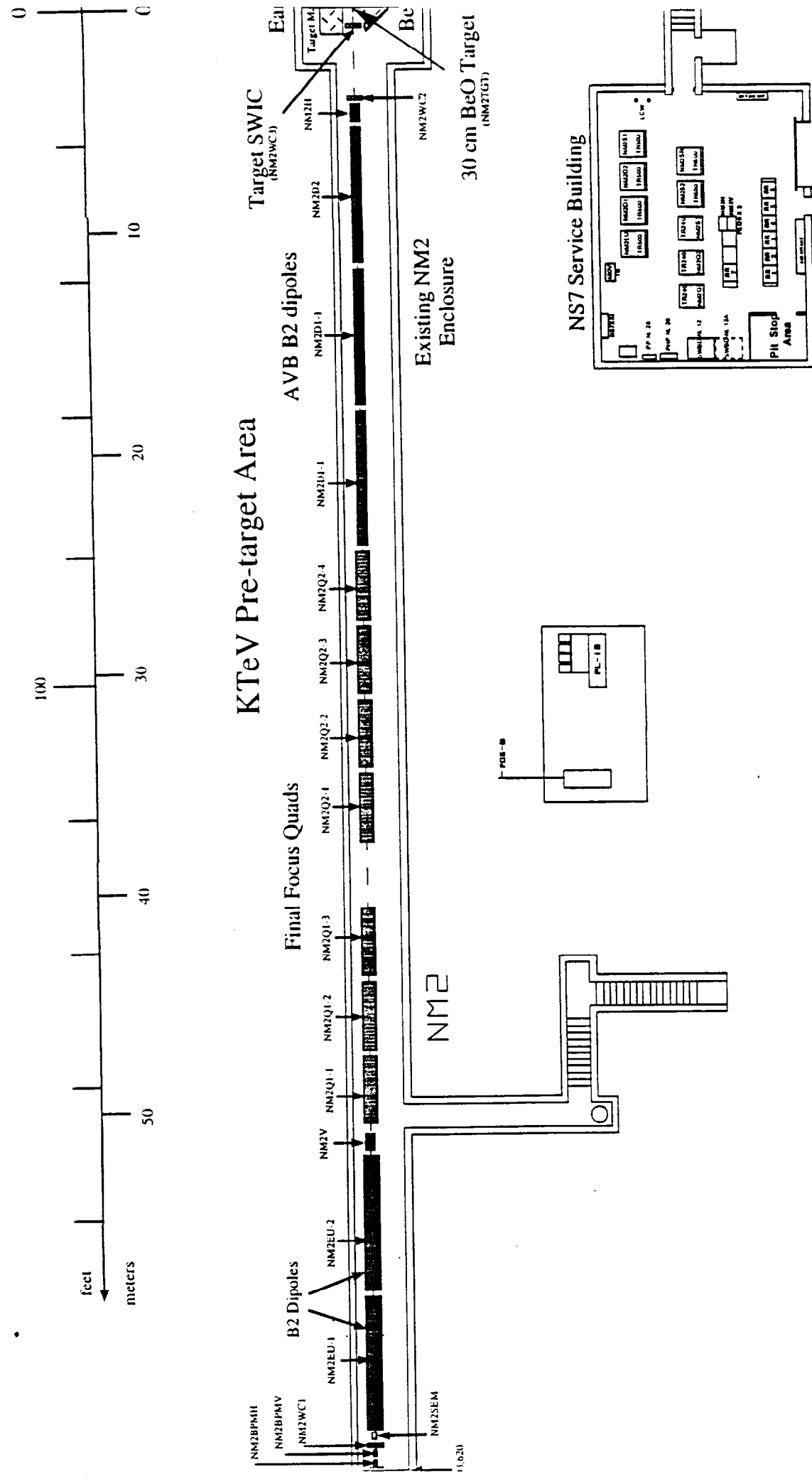


Figure 2.2.3 Magnet and instrumentation layout in enclosure NM2

### 2.3 The Angle Varying Bend (AVB) System

The vertical targeting angle can be changed using NM2D1 and NM2D2. Figure 2.3.1 shows a picture of the AVB system. The thicker line is the -4.00 mr beam trajectory; the thinner line is the -5.6 mr trajectory.

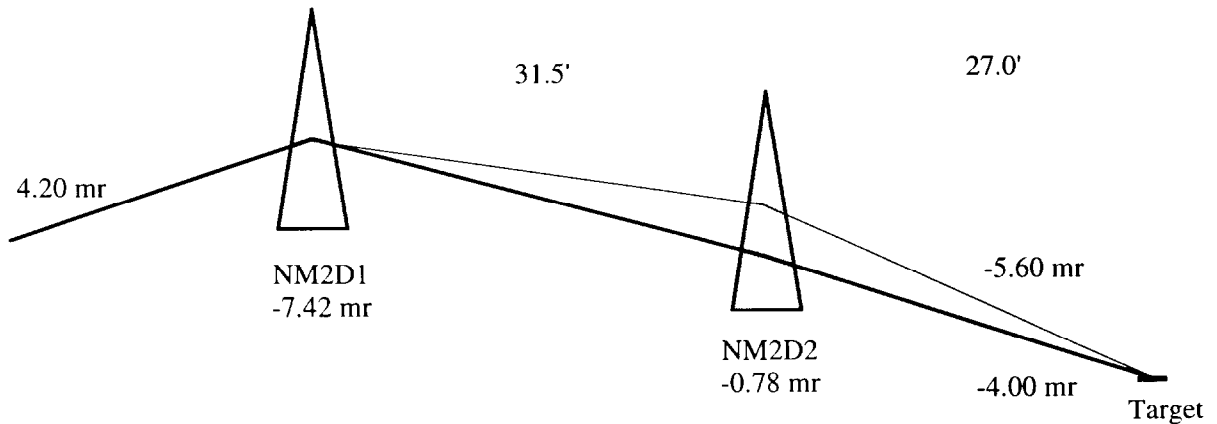


Figure 2.3.1  
AVB System Layout. The vertical and horizontal scales are different.

As can be seen in the figure, the angle is the smallest when NM2D2 is at its lowest field value. By increasing the NM2D2 field and at the same time decreasing NM2D1, the angle can be increased without changing the beam position at the target. The targeting angle is maximum when NM2D2 reaches its maximum. Then the bigger the NM2D2 range, the bigger the range in targeting angle. A range of 0 to 4800 amps was assumed for NM2D2 (a B2 magnet).

The beam is rising in front of the NM2D1 magnets. The NM2D1 and NM2D2 magnets are used to bend the beam down. At 900 GeV/c, the two B2s in the NM2D1 string are not enough to bend the beam down to the minimum angle required (-4.0 mr); therefore, the minimum value of NM2D2 must be greater than zero. If the minimum current of NM2D2 were to be reduced to zero, then the range of the AVB system would increase by 20%.

The criteria to choose the fields and positions of NM2D1 and NM2D2 were:

Maximum energy of 900 GeV.

Minimum targeting angle -4.0 mr.

Maximum current for NM2D1 and NM2D2 is 4800 amps.

At a targeting angle of -4.0 mr NM2D1 runs at its maximum current (4800 amps). This was done to maximize the AVB's range.

With the above criteria the range in vertical targeting angle is:

800 GeV/c: from -4.0 mr to -5.8 mr

900 GeV/c: from -4.0 mr to -5.6 mr

The magnets will be positioned for a maximum momentum of 900 GeV/c to increase the range of the AVB system.

## 2.4 Optics

### 2.4.1 Goals

The three goals that guided the design of the primary beam optics were:

To achieve the requested beam size.

To form a beam waist at the target.

To minimize the dispersion at the target.

The requested beam size is  $\sigma \leq 250 \mu\text{m}$  for both the horizontal and vertical beam profiles. A waist at the target will provide: a) minimum beam size change through the target, and b) beam size stability. Since the beam coming out of the Tevatron is not monochromatic, to achieve maximum position and angle stability the dispersion at the target needs to be minimized. As the reader follows the logic behind the design it will become clear that some compromises have to be made. For example, it is possible to have a waist at the target with almost no dispersion only if the beam size is substantially smaller than  $250 \mu\text{m}$ . Or, it is possible to have a  $250 \mu\text{m}$  beam and minimal dispersion only if there is no waist at the target.

## 2.4.2 Constraints

In trying to meet the above goals it was found that of all the constraints the main three are: a) the beam phase space, b) the beam as it comes from Switchyard, and c) the beam size at the NM2 quadrupoles. Beam phase space conservation is the strongest constraint. On the other hand this is the least known quantity in any beam design. The values of the emittance obtained by C. D. Moore et al. were used:  $\varepsilon_H = 8\pi \text{ mm } \mu\text{rad}$  horizontally, and  $\varepsilon_V = 6\pi \text{ mm } \mu\text{rad}$  vertically.<sup>11</sup> The emittance here is defined as  $\varepsilon = \sigma_x \sigma_y \pi \text{ mm } \mu\text{rad}$ .

There is a small amount of flexibility in changing the beam delivered by Switchyard. As can be seen in Figure 2.4.1, Q90 affects all three areas (Proton, Meson and Neutrino), Q100/Q101 affect both Meson and Neutrino, and Q106 affects the two Neutrino beams: E815 and KTeV. The last four quadrupoles, Q420, Q424, NM2Q1 and NM2Q2, only affect the KTeV beam. Of these four quadrupoles, two are in Switchyard enclosure G2 (Q420 and Q424) and two in enclosure NM2 (NM2Q1 and NM2Q2). The polarities and currents of these last four quads can be chosen as needed. Figure 2.4.2 shows the measured and predicted beam profiles for the neutrino area given by C.D. Moore et al. Figure 2.4.3 shows the  $R_{16}$  matrix element for the NM/KTeV line in units of mm/0.01% ( $R_{16}$  is known as the dispersion. If  $R_{16}=1$ , then a beam momentum change of  $\Delta p/p = 0.01\%$  will produce a beam motion of 1mm).

---

<sup>11</sup> "Tevatron Extraction Model," by C. D. Moore, R. Coleman, G. Goderre, M. Yang.

# KTeV Primary Beamline Optics from Switchyard Extraction to the NM2 Target

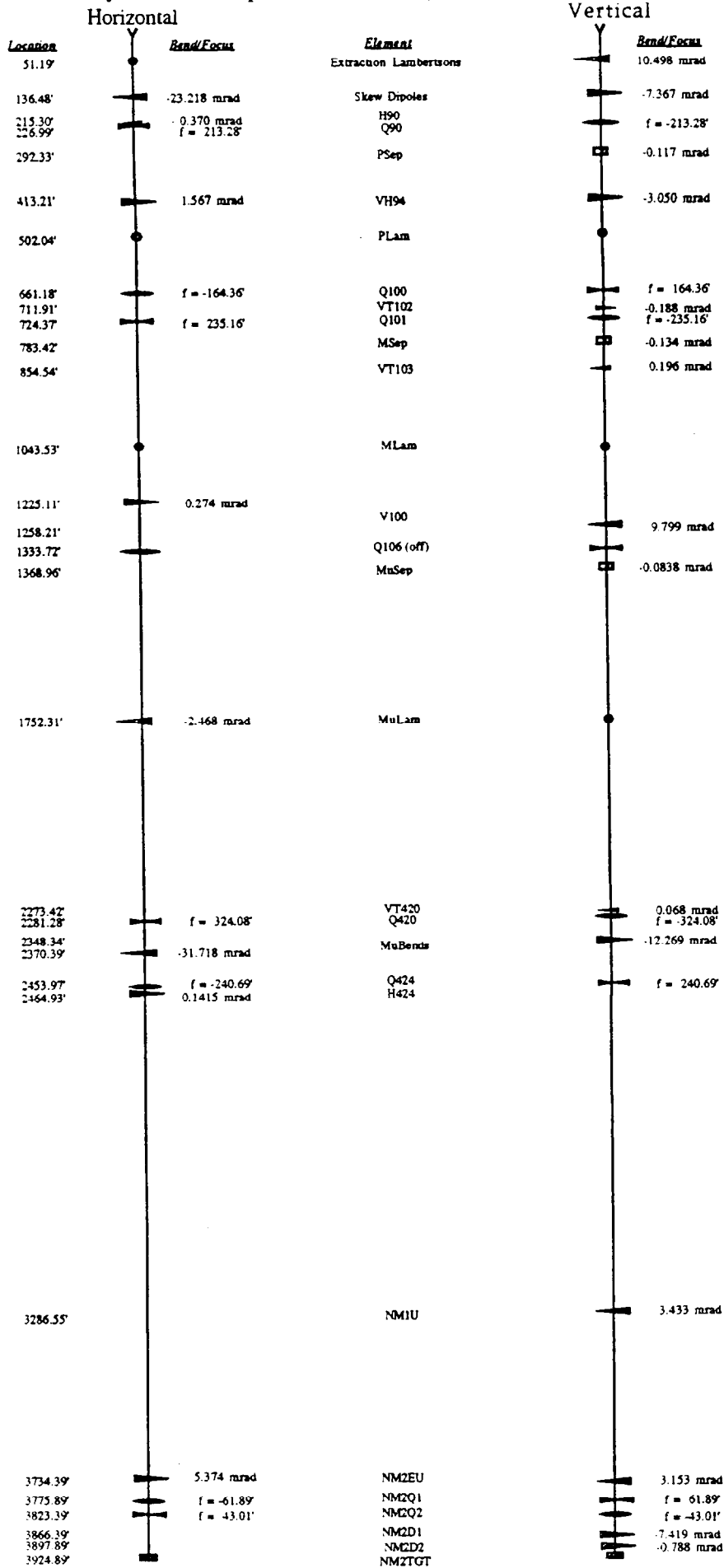


FIGURE 2.4.1.

Beam elements from A0 (Tevatron extraction point) to the KTeV target.  
The last element in Switchyard is the H424 trim.

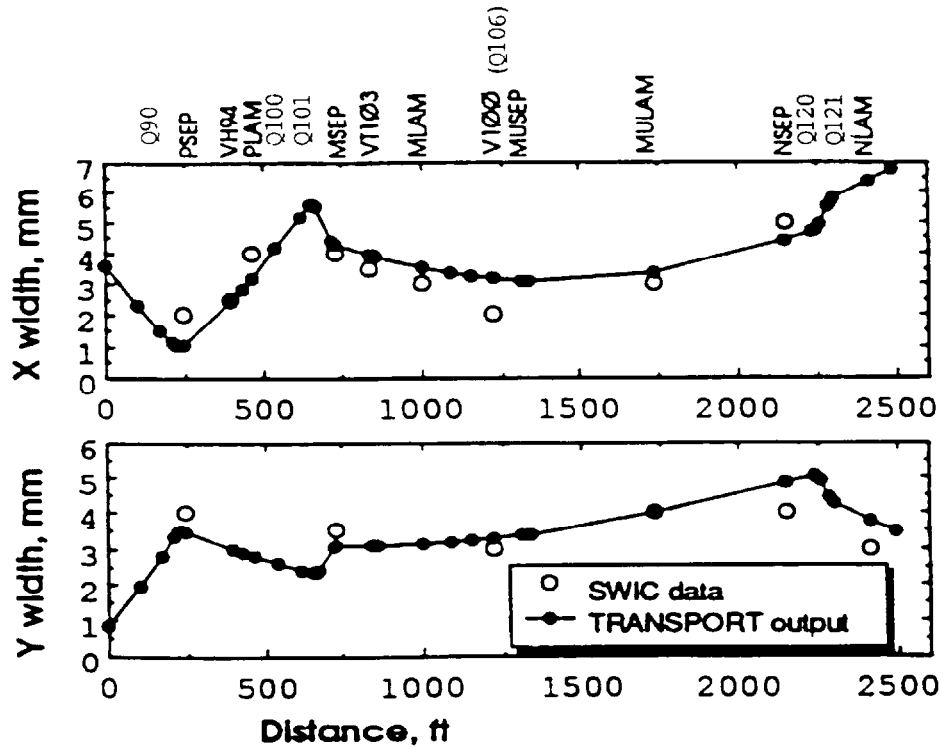


Figure 2.4.2  
 Measured and predicted beam profiles for the neutrino area as given by  
 C.D. Moore et al.

For a waist at the target, the beam size at the last set of quadrupoles is determined by the emittance. Using an emittance of  $8\pi \text{ mm } \mu\text{rad}$  and a beam size of  $250 \mu\text{m}$ , the beam size 100 feet upstream of the target will have to be about  $\sigma = 1 \text{ mm}$  (that is  $(8/0.25)$  microradians times 100 feet).

### 2.4.3 Options

The value of  $R_{16}$  in G2 can be controlled using the Q100 and Q101 quadrupoles<sup>12</sup>. If the dispersion is non zero at the Q420-Q424 G2 quadrupoles (see Figure 2.4.3), then these two quadrupoles can be used to focus the dispersion into NM2. If the dispersion is very close to zero in NM2, then

<sup>12</sup> The change in the currents is of the order of 5%. Studies show that this change has minimal effect in Meson and Neutrino.

NM2Q1 and NM2Q2 will have little effect on it, and therefore it will remain very close to zero. To focus the dispersion, Q420 and Q424 would have to run at a higher current, producing an intermediate focus between G2 and NM2 (see Figure 2.4.4). This produces a large beam at NM2Q1 and, consequently, a very small beam size at the target waist. There can be target heating problems if the beam size at the target is too small.

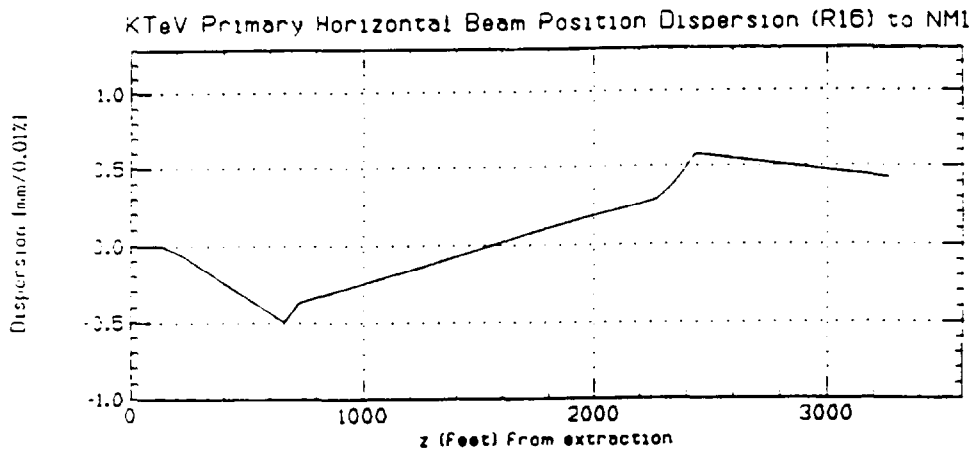


Figure 2.4.3

Dispersion ( $R_{16}$  matrix element) from A0 to NM1. The units are mm/0.01%.

If the dispersion is not minimized, then the G2 quads can be used to produce a smaller beam in NM2 and therefore a larger beam size at the target waist (see Figure 2.4.7). The beam sizes are very small everywhere but the dispersion has increased.

Figure 2.4.8 shows a case in which the dispersion at the target is close to zero. A disadvantage of this solution is a bigger beam at NM2Q1, and therefore a much smaller beam at the horizontal waist. A bigger beam has the potential to produce unwanted muons by scraping in the magnets. If the beam is too small, target heating problems are a risk. Again, the vertical beam size was chosen to satisfy the requirement  $\sigma_x \sigma_y \approx 0.025 \text{ mm}^2$ .

To select the quadrupole's polarity, the options described above must be kept in mind. The G2 quads should be effective to focus the dispersion and to keep the beam size at the target waist at a reasonable level. To satisfy this,

Q420 has to be defocusing and Q424 to be focusing. This will increase the dispersion going from Q420 to Q424 but at the same time it will make the quadrupoles more effective. For the quadrupoles in NM2, the farthest upstream quadrupole has to be focusing to keep the beam from getting too small and unstable at the target waist. Then NM2Q1 will be focusing and NM2Q2 defocusing.

#### 2.4.3.1 About the Dispersion

The term "minimize the dispersion" should be quantified. The momentum spread in the Tevatron during collider run is  $\Delta p/p \approx 0.38 \times 10^{-4}$  at 95%<sup>13</sup>. Taking into account the increase of momentum spread with increasing intensity, a momentum spread of  $\Delta p/p = 0.5 \times 10^{-4}$  is used. Then for a beam motion of less than 100 microns and 25 microradians, the dispersion should be less than two meters and 0.5 radians. In units of mm/0.01% and  $\mu\text{r}/0.01\%$  this translates to  $R_{16} \leq 0.1$  and  $R_{26} \leq 20$ .

#### 2.4.3.2 Matching with the Tevatron Lattice

The Tevatron lattice for fixed target has a dispersion at A0 of 2.5 meters and -0.028 radians<sup>14</sup>. Thus the TRANSPORT input file was started at A0 with these values for the dispersion. Another consideration could be to make an achromatic transfer from the D0 extraction septa to the KTeV target. As this problem is not well enough understood, work should continue in this area.

Figures 2.4.4, 2.4.5 and 2.4.6 show cases with and without the Tevatron dispersion. As can be seen in this plot there is some control over the dispersion using Q100 and Q101. The changes in these quadrupoles are of the order of 5% and the effect that these changes have on the Meson area are minimal.

---

<sup>13</sup> C. Hojvat, Stan Pruss and G. Jackson, private communication.

<sup>14</sup> Extracted from a SYNCH output provided by Al Russell.

#### 2.4.4 Design

Our choice for the optics is given in Figure 2.4.4. In this case the smallest distance, measured in beam widths, between the center of the beam and the face of a magnet is about 7 sigma. The beam forms a horizontal waist at the target. The vertical beam size was chosen such that  $\sigma_x \sigma_y \approx 0.025 \text{mm}^2$ . This last number is set by target heating<sup>15</sup>. Referring to Figure 2.4.4., the dispersion calculations are  $R_{16} \Delta p/p \approx 50 \mu\text{m}$  and  $R_{26} \Delta p/p \approx 3 \mu\text{rad}$ . As mentioned above, the momentum spread in the Tevatron is about  $\Delta p/p \approx 0.5 \times 10^{-4}$  at 95%.

---

<sup>15</sup> During start up, the Run Conditions will only allow low intensity. Among other things this will protect the target. If beam studies show that the beam can be too small, we will narrow the windows in the NM2Q1 and NM2Q2 current interlocks to protect the target.

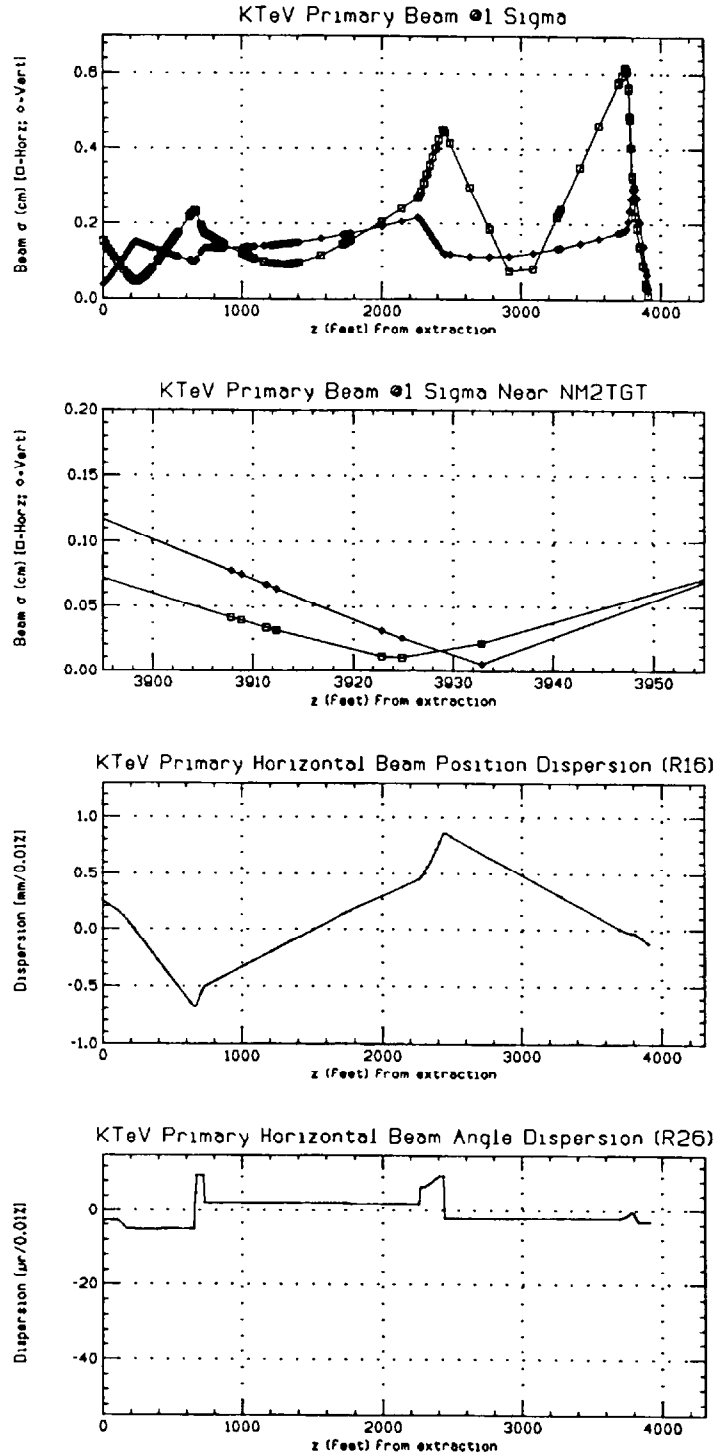


Figure 2.4.4 Beam profile (sigma) from A0 to the target, b) beam profile in the target region (target at  $z=3925'$ ), c) R16 and d) R26. The requirements at the target were a waist in  $x$  and .25mm in  $y$ , and the minimization of the dispersion. Q100 and Q101 were changed by 7.8% and 6.1% respectively; these changes have very little effect in the vertical plane.

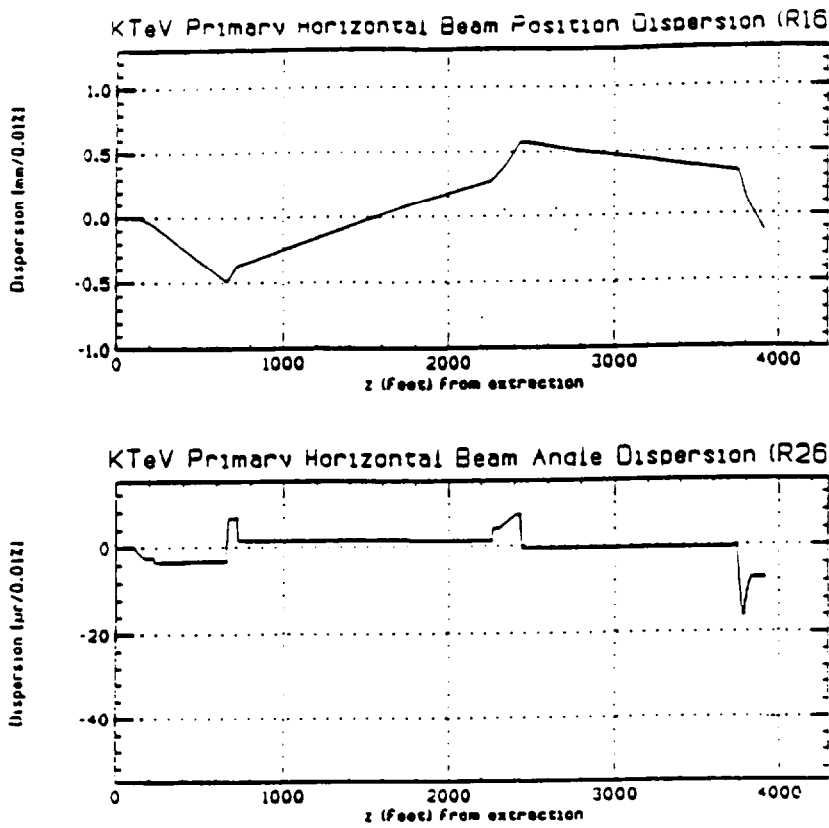


Fig. 2.4.5: a) R<sub>16</sub> and b) R<sub>26</sub> for zero Tevatron dispersion and no changes in Q<sub>100</sub> and Q<sub>101</sub>. All the other magnet currents are the same as in Fig. 2.4.4.

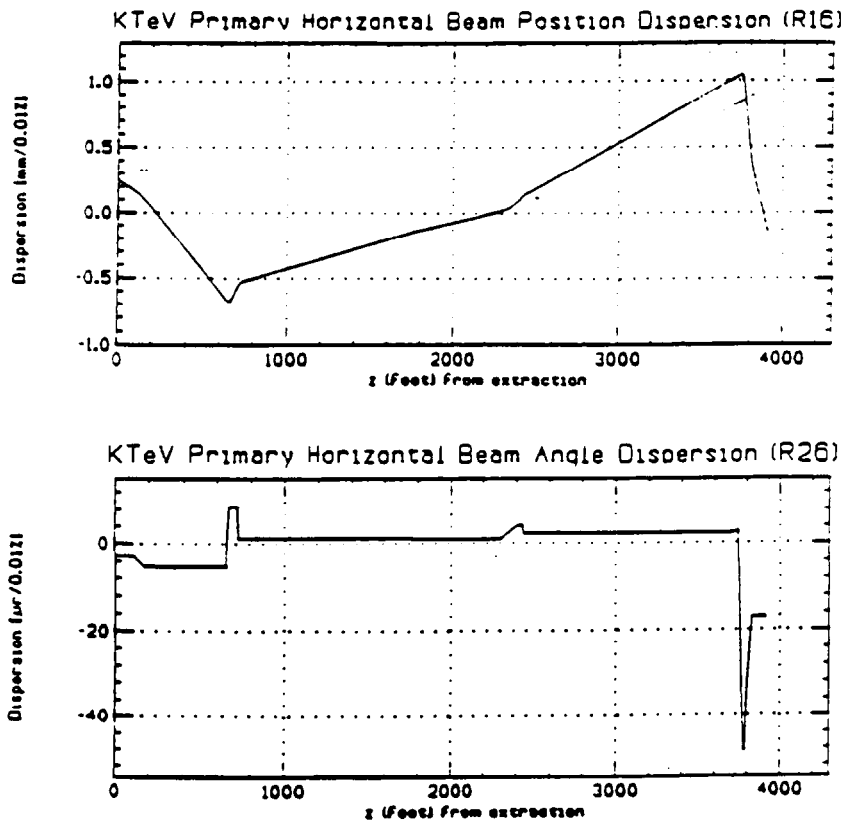


Fig. 2.4.6: a) R<sub>16</sub> and b) R<sub>26</sub> for Tevatron dispersion matching and no changes in Q<sub>100</sub> and Q<sub>101</sub>. All the other magnet currents are the same as in Fig. 2.4.4.

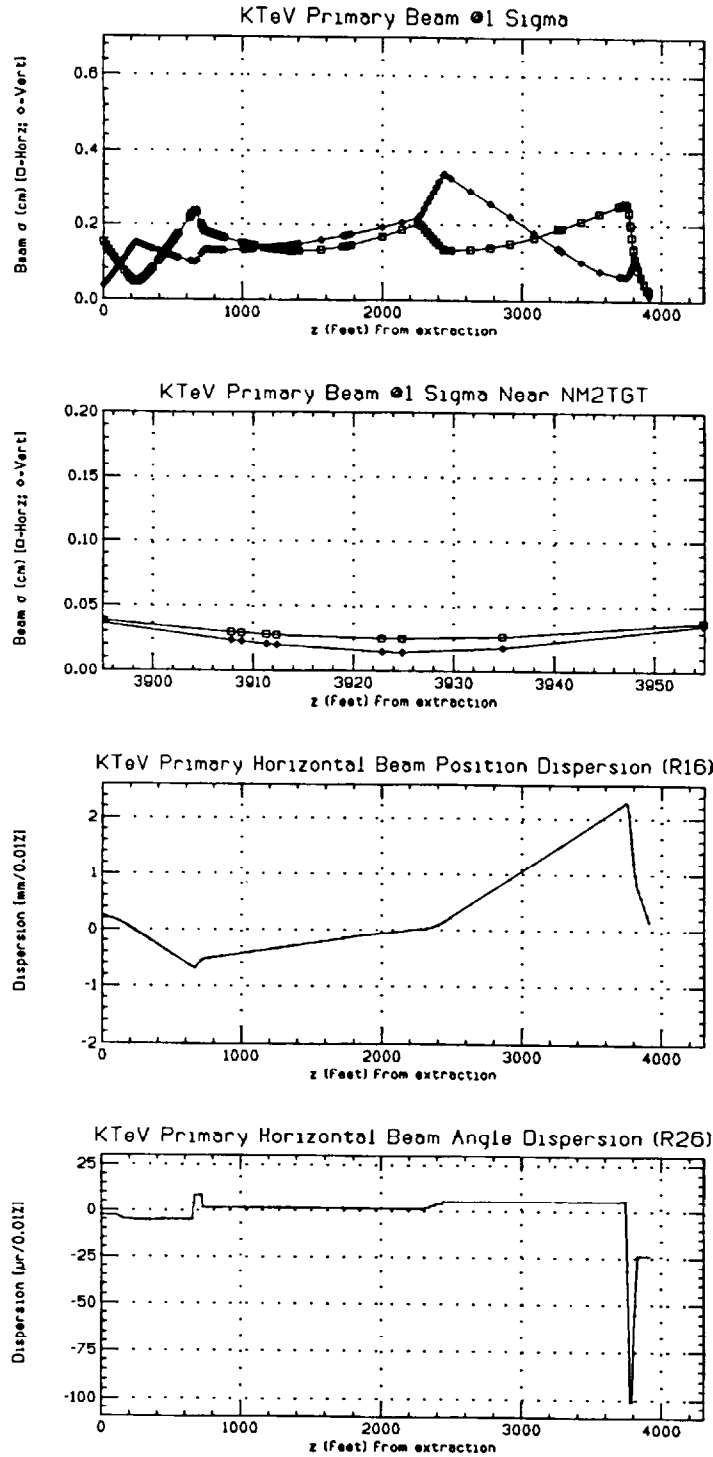


Figure 2.4.7

Beam profile (sigma) from A0 to the target, b) beam profile in the target region (target at  $z=3925'$ ), c) R<sub>16</sub> and d) R<sub>26</sub>. The requirements at the target were a beam waist and maximization of the beam size at the waist. No changes were made to Q100 and Q101.

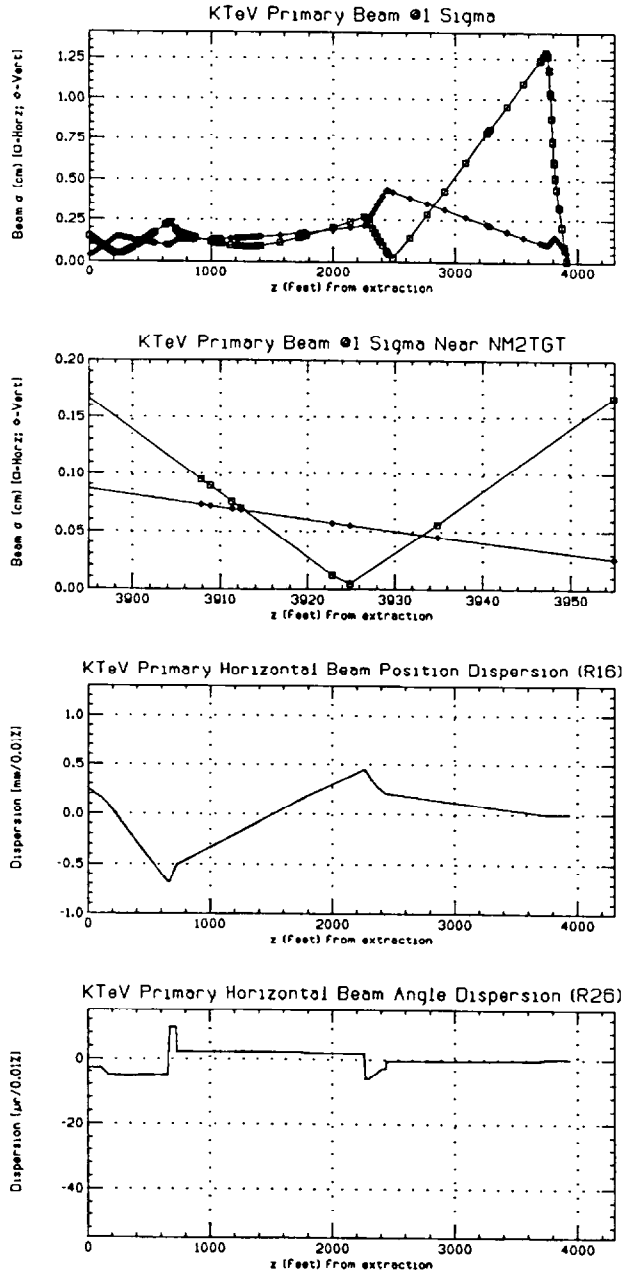


Figure 2.4.8

Beam profile (sigma) from A0 to the target, b) beam profile in the target region (target at  $z=3925'$ ), c) R16 and d) R26. The quadrupoles in these plots have the same polarities as those in Fig. 2.4.7. But the requirements at the target were a waist in x and 0.55mm in y, and the minimization of the dispersion. Q100 and Q101 were changed by 7.8% and 6.1% respectively; these changes have very little effect in the vertical plane.

Table 2.4.9  
Quadrupole Gradients

Quadrupole	Figure 2.4.3	Figure 2.4.4	Figure 2.4.7	Figure 2.4.8
Q100	2.9744	3.2056	2.9744	3.2056
Q101	-3.0808	-3.2688	-3.0808	-3.2688
Q420	-2.2397	-2.2397	2.0901	2.0251
Q424	3.0525	3.0525	-2.0953	-2.0726
NM2Q1	3.9032	3.9032	3.7133	3.3060
NM2Q2	-4.0036	-4.0036	-4.0761	-2.8599

Table of quadrupole gradients (in KG/inch) for the figures in this section. Figures 2.4.5 and 2.4.6 have the same quadrupole gradients as Figure 2.4.3. The beam energy is 800 GeV.

Table 2.4.10  
Quadrupole Currents

Quadrupole	Figure 2.4.3	Figure 2.4.4	Figure 2.4.7	Figure 2.4.8
Q100	60.0	61.4	60.0	61.4
Q101	-59.0	-62.6	-59.0	-62.6
Q420	-42.9	-42.9	40.0	38.8
Q424	58.5	58.5	-40.1	-39.7
NM2Q1	750.1	750.1	713.6	635.3
NM2Q2	-769.4	-769.4	-783.3	-549.6

Table of quadrupole currents (in Amps) for the figures in this section. Figures 2.4.5 and 2.4.6 have the same quadrupole currents as Figure 2.4.3. The beam energy is 800 GeV.

## 2.5 Stability

### 2.5.1 Sources of Instabilities

There are four sources of instabilities:

The beam moves as it is extracted from the accelerator.

The current of the magnets between extraction and the KTeV target changes with time. This can be due to:

- Power supply instabilities
- Small adjustments due to changes in beam splits or beam extraction.

Changes in beam splits.

The position monitoring devices move with time.

The beam instabilities can be classified in two groups: 1) slow instabilities, or beam motion over a period of a few or more spills, and 2) beam roll, or beam motion during the spill.

The plan to cancel the slow instabilities is to use EPICURE (Research Division's beam control system) to monitor the beam position at different SWICs and to make small corrections in the magnet's currents to keep the beam stable. EPICURE can be used to make these corrections on a spill by spill basis. What is needed for this strategy to work is: a) reasonably stable power supplies (thus avoiding making changes in every spill), b) enough sensitivity in the magnets to make small corrections, c) stable beam instrumentation, and d) reliable read-back of the instrumentation. The first three issues will be examined in the following subsections.

Beam roll can be produced by changes in beam momentum, position or slope during extraction. It can also be produced by poor magnet regulation after beam extraction, but the known regulation of the magnets between extraction and the KTeV target is compatible with the required beam stability (see the following section). The effects of beam motion at extraction due to small changes in momentum was covered in the previous section under the dispersion studies. If the beam position and/or slope at extraction were to change during the spill, the plan to cancel its effects on the KTeV target is to

use in a closed loop two Switchyard magnets (MuLam and H424) to keep the beam stable at two positions (the downstream end of G2 and the upstream end of NM2). The reasons for this are: a) ACNET (Switchyard's beam control system) can make several corrections during the spill, b) during the period of one spill all the instrumentation is very stable, and c) only a quarter of a millimeter beam stability at the downstream end of G2 and the upstream end of NM2 is needed in order to have 50 microns stability at the KTeV target. The details will be examined in the Beam Roll subsection.

### 2.5.2 Power Supply Stability

Table 2.5.1 shows the change in beam position and angle at the target when the dipoles' field is changed by 100 ppm ( $10^{-4}$ ). The main bends between A0 and the target are shown in the table. The contributions of the dipoles and quadrupoles not shown in the table are very small. The units are microns and microradians.

Table 2.5.1  
Change in Beam Position and Angle

Magnet	$\Delta x$ ( $\mu\text{m}$ )	$\Delta \dot{x}$ ( $\mu\text{rad}$ )	$\Delta y$ ( $\mu\text{m}$ )	$\Delta \dot{y}$ ( $\mu\text{rad}$ )
Ex. Lamb.	0	0	-10	2
SKDP	21	-6	5	1
VH94	-2	-1	2	2
V100	0	0	55	-25
MULAM	-5	1	0	0
MUBEND	148	15	-108	43
NM1U	0	0	11	-3
NM2EU	-41	-1	6	0
NM2D1	0	0	-13	-1
NM2D2	0	0	-1	0

There are four magnets that have large contributions: SKDP, MUBEND and NM2EU and V100. Both SKDP and MUBEND are superconducting magnets and with a HOLEC transducer can regulate to 20 - 50 ppm<sup>16</sup>. NM2EU is a regular magnet. Studies performed on beam motion during the last fixed target run with NE9E show that regular power supplies

<sup>16</sup> A. Visser, M. Coburn, private communication.

regulate to better than 150 ppm over a period of days (see Figure 2.7.1). Studies performed on NEFE with a hall probe show that between the beginning and the end of the spill those magnets were stable to better than 100 ppm. As in NM2EU, the magnets of the NE9E and NEFE strings are B2s. The fact that the regulation of NM2EU is close to the requested 100 microns position stability means that close attention must be paid to the power supply that will run that magnet. If needed, NM2EU can be run without ramping<sup>17</sup>. The V100 string does not have a HOLEC transducer, so its contribution may approach the 100 microns level.

### 2.5.3 Canceling Slow Instabilities

Slow instabilities are those that occur over a few or more spills. Examples of these are the small adjustments made to magnets due to changes in beam splits or beam extraction. To correct these instabilities, the beam position will be measured every spill and, if necessary, corrections will be made by computer to magnet currents between spills. To do this, the relation between a current change in a magnet and the beam position change in a SWIC has to be known. Throughout this section, the word "SWIC" will refer to beam position monitors in general, although the beam position monitors can be a BPM or other beam position measuring device.

KTeV requires careful control of the primary beam from the upstream end of enclosure NM1 to the target, located in NM2. Currently, KTeV is able to control and monitor all devices from enclosures NM1 to the target via the EPICURE control system. However, in order to use Epicure to control the position of the beam at the upstream end of NM1, Epicure control has been extended to the switchyard magnets VT420 and H424.

Figure 2.5.1 illustrates a conceptual layout of the magnets and SWIC's from VT420 to the target. As can be seen in the figure, there are four SWICs to measure beam position: NM1WC, NM2WC1, NM2WC2 and NM2WC3. Each one will be used to measure vertical and horizontal beam positions. There are nine dipoles to make beam corrections: VT420, H424, NM1U,

---

<sup>17</sup> Leon Beverly, private communication.

NM1H, NM2EU, NM2V, NM2D1, NM2D2 and NM2H. Note that the MuBends (a large cryogenic string) are not included. The relation between the changes in the dipole's field and the changes in beam position at the SWICs is linear. The following matrix gives such a relation in units of microns per gauss. A beam energy of 1 TeV is assumed.

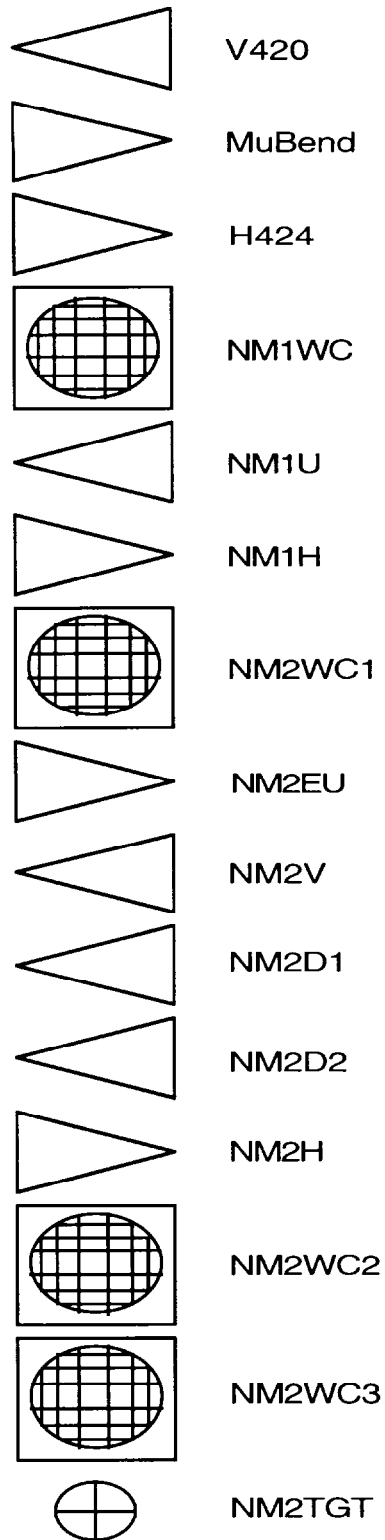


Figure 2.5.1  
 SWIC's and Magnets used in Calculating Tuning Matrices  
 (Schematic - not to scale)

$$\begin{pmatrix} \text{H424Vs} \\ \text{NM1WCV} \\ \text{NM2WC1V} \\ \text{NM2WC2V} \\ \text{NM2WC3V} \\ \text{NM2TGTV} \\ \text{H424Hs} \\ \text{NM1WCH} \\ \text{NM2WC1H} \\ \text{NM2WC2H} \\ \text{NM2WC3H} \\ \text{NM2TGTH} \end{pmatrix} = \begin{pmatrix} 0 & -0.39 & 0 & 0 & 0 & 0 & 0 & 0 & 0 & 0 \\ -0.15 & -12.9 & 0 & 0 & 0 & 0 & 0 & 0 & 0 & 0 \\ -0.23 & -19.0 & 23.7 & 0 & 0 & 0 & 0 & 0 & 0 & 0 \\ -0.08 & -6.94 & 11.6 & -0.437 & -5.12 & -0.81 & 0 & 0 & 0 & 3.89 \\ -0.04 & -3.41 & 6.80 & -0.422 & -6.29 & -1.39 & 0 & 0 & 0 & 3.53 \\ -0.03 & -2.74 & 5.89 & -0.419 & -6.52 & -1.50 & 0 & 0 & 0 & 3.47 \\ 78.5 & 0 & 0 & 0 & 0 & 0 & 0 & 0 & 0 & 0 \\ -17.5 & 0 & 0 & 0 & 0 & 0 & -22.6 & 0 & 0 & 0 \\ -71.9 & 0 & 0 & 0 & 0 & 0 & -34.7 & -2.88 & 0 & 0 \\ -8.68 & 0 & 0 & 0 & 0 & 0 & 2.96 & -0.79 & -0.016 & -21.9 \\ -6.00 & 0 & 0 & 0 & 0 & 0 & 4.86 & -0.71 & -0.089 & -23.9 \\ -5.49 & 0 & 0 & 0 & 0 & 0 & 5.21 & -0.70 & -0.103 & -24.3 \end{pmatrix} \begin{pmatrix} \text{MuLam} \\ \text{VT420} \\ \text{NM1U} \\ \text{NM2V} \\ \text{NM2D1} \\ \text{NM2D2} \\ \text{H424} \\ \text{NM1H} \\ \text{NM2H} \\ \text{NM2EU} \end{pmatrix}$$

For beam control, the beam position is measured and changes are made to the magnet currents. Therefore, the previous matrix has to be inverted. Only square matrices can be inverted. The beam position at H424 is controlled by Switchyard, therefore it will not be included in the calculations. NM2TGT will not be included either because there is no instrumentation there. If the beam position at H424 is not going to be controlled then MuLam is not needed. As a control device either NM2D1 or NM2D2 can be used to make vertical corrections at the target. After eliminating rows one, six, seven and twelve, and columns one and five, the matrix can be inverted. The result is:

$$\begin{pmatrix} \text{VT420} \\ \text{NM1U} \\ \text{NM2V} \\ \text{NM2D2} \\ \text{H424} \\ \text{NM1H} \\ \text{NM2H} \\ \text{NM2EU} \end{pmatrix} = \begin{pmatrix} -0.0775 & 0 & 0 & 0 & 0 & 0 & 0 & 0 \\ -0.0621 & 0.0422 & 0 & 0 & 0 & 0 & 0 & 0 \\ -0.471 & 1.67 & -5.19 & 3.00 & -0.240 & 0.123 & -0.538 & 0.0954 \\ 0.0291 & -0.301 & 1.57 & -1.63 & 0.0087 & -0.00442 & 0.0196 & -0.00347 \\ 0 & 0 & 0 & 0 & -0.0443 & 0 & 0 & 0 \\ 0 & 0 & 0 & 0 & 0.534 & -0.347 & 0 & 0 \\ 0 & 0 & 0 & 0 & 0.0320 & -0.678 & 15.2 & -13.9 \\ 0 & 0 & 0 & 0 & -0.0251 & 0.0129 & -0.0565 & 0.0100 \end{pmatrix} \begin{pmatrix} \text{NM1WCV} \\ \text{NM2WC1V} \\ \text{NM2WC2V} \\ \text{NM2WC3V} \\ \text{NM1WCH} \\ \text{NM2WC1H} \\ \text{NM2WC2H} \\ \text{NM2WC3H} \end{pmatrix}$$

In the range we work, the relation between current and field is linear. Because the relation between field and position is also linear (for small changes), a matrix that will relate the changes in magnet currents and beam positions can be obtained.

The question of accuracy of control is now addressed. That is, given the minimum current change what is the smallest beam position change that can be made? Table 2.5.2 summarizes the relevant information to do the calculation. Magnet currents and fields were calculated for 1 TeV.

Table 2.5.2  
Summary of Parameters Pertinent to Control System

Magnet	Type	Nominal			d(field)/	Maximum	Minimum Change	
		Field	Current	Bend	d(current)		Current	Current
		[kG]	[Amp]	[mradian]	[G/Amp]	[Amp]	[Amp]	[Gauss]
V420	3.5-2-35	2.57	65	-0.0684	396.0	200	0.00610	2.42
H424	EPB	1.55	148	0.141	10.5	1700	0.0763	0.801
NM1U	EPB	18.80	2075	3.430	3.8	1700	0.0763	0.290
NM1H	4-4-30	0.00	0	0.000	25.0	200	0.00610	0.153
NM2EU	B2	17.05	4414	6.23	3.42	5000	0.153	0.522
NM2V	4-4-30	0.00	0	0.000	25.0	200	0.00610	0.153
NM2D1	B2	20.30	5293	7.42	2.14	5000	0.153	0.327
NM2D2	B2	4.31	1399	0.778	3.90	5000	0.153	0.595
NM2H	4-4-30	0.00	0	0.000	25.0	200	0.00610	0.153

Because some magnets are run near saturation, the relation between current and field varies between magnets (c.f. H424 and NM1U). The minimum change in the current was calculated assuming the 15 bit precision of an 1151 power supply reference card<sup>18</sup>. The change in field due to a change in current was calculated at the fields specified in the Field column. Note that currents for some magnets are calculated to be above the maximum power supply current—this is because all work is done at 1000 GeV, whereas the actual beam will be 800 GeV or 900 GeV.

<sup>18</sup>Although the 1151 has a 16 bit register, the current firmware only supports 15 bit precision. See "RD Controls Hardware Release Note 26.0".

From this information, the minimum change at NM2WC3 can also be predicted. Table 2.5.3 summarizes this information (note that units for motion are micrometers). Blanks indicate no coupling.

Table 2.5.3  
Minimum change at NM2WC3

SWIC	Magnet								
NM2WC3	V420	NM1U	NM2V	NM2D1	NM2D2	H424	NM1H	NM2H	NM2EU
Vertical	8.2	2.0	0.064	2.1	0.83				1.8
Horizontal						3.9	0.12	0.014	12.0

Minimum change, in micrometers, at NM2WC3, for KTeV primary beamline magnets.

The above table shows that adequate control of the beam is possible. The EPICURE software to read beam positions every spill and make magnet corrections between the spills was developed and tested in the Neutrino primary beams during the last Fixed Target run. For the next Fixed Target run, this software will be extended to run in all beam lines, including KTeV.

#### 2.5.4 SWIC Stability

The stability requirements for each of the SWICs determine which SWICs to use for beam control. If there are no magnets between the SWICs or between the SWICs and the target, then the SWIC's stability is the only relevant issue. If there are magnets in between, then their stability also becomes an issue. Three cases will now be explored, one without and two with magnets in between the instrumentation or the target.

**Case 1:** There are no magnets between NM2WC2 and the target. For purposes of the calculation, NM2WC2 is 12.5 feet from the target and NM2WC3 is 2 feet. Thus, in units of microns and microradians:

$$\begin{pmatrix} x_T \\ \dot{x}_T \end{pmatrix} = \begin{pmatrix} -0.190 & 1.19 \\ -0.312 & 0.312 \end{pmatrix} \begin{pmatrix} x_{NM2WC2} \\ x_{NM2WC3} \end{pmatrix}$$

Assuming that NM2WC2 and NM2WC3 move independently, the error contributions must be added in quadrature. For example:

$$\Delta x_T = \sqrt{(-0.190 \cdot \Delta x_{NM2WC2})^2 + (1.19 \cdot \Delta x_{NM2WC3})^2}$$

Thus a 40 $\mu\text{m}$  stability in NM2WC2 and NM2WC3 will provide a 50 $\mu\text{m}$  stability in beam position and 18 $\mu\text{rad}$  stability in beam angle.

**Case 2:** Assuming that the magnets in NM2 are perfectly stable, then the SWICs, NM1WC and NM2WC1, can be used for beam control. This is a good assumption for all the magnets except NM2EU (see Section 2.5.2). The relation of the SWIC's motion and the beam motion at the target in units of microns and microradians is given by:

$$\begin{pmatrix} x_T \\ \dot{x}_T \end{pmatrix} = \begin{pmatrix} -0.591 & 0.246 \\ -0.014 & -0.008 \end{pmatrix} \begin{pmatrix} x_{NM1WC} \\ x_{NM2WC1} \end{pmatrix}$$

Moving one SWIC at a time, it is noted that if  $\Delta x_T \leq 50\mu\text{m}$ , then  $\Delta x_{NM1WC} \leq 85\mu\text{m}$  and  $\Delta x_{NM2WC1} \leq 200\mu\text{m}$ . The angular stability is better than a microradian.

**Case 3:** Assuming that the magnets in NM1 and NM2 are perfectly stable, then H424 (the last SWIC in G2) and NM2WC1 can be used for beam control. Horizontally there is only a trim in NM1, so NM1 should not contribute to the beam motion. The relation of the SWICs motion and the beam motion at the target in units of microns and microradians is given by:

$$\begin{pmatrix} x_T \\ \dot{x}_T \end{pmatrix} = \begin{pmatrix} -0.202 & -0.144 \\ -0.005 & -0.017 \end{pmatrix} \begin{pmatrix} x_{H424} \\ x_{NM2WC1} \end{pmatrix}$$

Moving one SWIC at a time, it is noted that if  $\Delta x_T \leq 50\mu\text{m}$ , then  $\Delta x_{H424} \leq 250\mu\text{m}$  and  $\Delta x_{NM2WC1} \leq 350\mu\text{m}$ . The angular stability is better than a microradian.

To calculate the last two matrices the following transfer matrix between NM2WC1 and the target was used:

$$\begin{pmatrix} x_T \\ \dot{x}_T \end{pmatrix} = \begin{pmatrix} -0.34549 & 74.4209 \\ -0.021688 & 1.77726 \end{pmatrix} \begin{pmatrix} x_{NM2WC1} \\ \dot{x}_{NM2WC1} \end{pmatrix}$$

This corresponds to the solution of Figure 2.4.4. The units are microns and microradians. The distances between SWICs is: 413 ft. from NM1WC to NM2WC1, and 1209 ft. from H424 to NM2WC1.

Over short periods of time, Case 3 is the preferred one. Over long periods it is not certain whether NM2EU will not change by more than 100 ppm, nor is it certain that two enclosures separated by 1200' (G2 and NM2) will not have relative horizontal displacements of more than a quarter of a millimeter. Therefore, Case 1 is recommended for the slow instabilities and Case 3 for the beam roll.

### 2.5.5 Beam Roll

This is the plan to correct for beam roll. If the beam position at H424 and NM2WC1 is measured with a precision of 50 microns (achievable using BPMs) and Case 3 of the previous section is used, then a stability at the target of 15 microns in beam position and 1 microradian in beam angle should be achievable.

To correct for beam roll, the beam position at H424 and NM2WC1 will be measured and the magnets H424 and MuLam will be used to keep the beam stable at the previous positions. This loop will be closed adapting software that already exists in ACNET. The ACNET beam control system is capable of making several corrections during the spill.

The transfer matrices from A0 (extraction) to the target give an idea of the beam stability required at extraction. The following transfer matrices correspond to Figure 2.4.4. The units are microns and microradians.

$$\begin{pmatrix} x_T \\ \dot{x}_T \end{pmatrix} = \begin{pmatrix} -0.0137 & 4.252 \\ -0.1876 & -14.72 \end{pmatrix} \begin{pmatrix} x_{A0} \\ \dot{x}_{A0} \end{pmatrix} \quad \begin{pmatrix} y_T \\ \dot{y}_T \end{pmatrix} = \begin{pmatrix} -0.1151 & -12.21 \\ 0.1183 & 3.860 \end{pmatrix} \begin{pmatrix} y_{A0} \\ \dot{y}_{A0} \end{pmatrix}$$

For example, the following equation shows that the beam stability at the target is more dependent on angular stability at extraction than on positional stability at extraction:

$$\Delta x_T = \sqrt{(-0.0137 \cdot \Delta x_{A0})^2 + (4.252 \cdot \Delta \dot{x}_{A0})^2}$$

Thus, a 1 micron movement at extraction results in an 0.0137 micron movement at the target, whereas a 1 microradian movement at extraction results in a 4.252 micron movement at the target.

## 2.5.6 Conclusions

Table 2.5.4 shows a summary of Cases 1 and 3 of the subsection on SWICs stability:

Table 2.5.4  
Summary of Cases 1 and 3

Parameter	Case 1	Case 3
Beam position stability	25 $\mu m$	15 $\mu m$
Beam angle stability	10 $\mu rad$	1 $\mu rad$
Required instrumentation stability	40 $\mu m$	250 $\mu m$
Assumes magnet stability	No	Yes
Separation between instrumentation	10'	1200'
Needed instrumentation position resolution	20 $\mu m$	50 $\mu m$

Angular and positional stability are calculated assuming stable instrumentation.

Case 3 relies on BPMs to measure beam position. Short BPMs can achieve a resolution of 50 microns at beam intensities of  $3 \times 10^{12}$  protons per pulse. Case 1 relies on new instrumentation to measure the beam position. The expected resolution of the new instrumentation is 20 microns (see section 2.7).

Case 3 is clearly better if one assumes that both the instrumentation and the magnets are stable. In the time scale of a few pulses this is certainly true. This is why the plan is to correct beam roll in this way. Over longer periods of time, it may be easier to keep NM2WC2 and NM2WC3 stable to 40 microns relative to the KTeV detector than to keep H424 and NM2WC1 stable to a quarter of a millimeter relative to each other and to the KTeV detector. Case 1 does not assume any special magnet stability. This is an advantage because to achieve a beam position stability of 50 microns at the target,

NM2EU needs to be stable to 125 parts per million (see subsection on Magnet Stability).

Case 3 will then be used for fast corrections and Case 1 for slow ones. It should be mentioned again that since Case 3 uses ACNET the capability for making fast corrections already exists.

## 2.6 Target Scans

Table 2.6.1 illustrates the beam scan capabilities at the target. "Position scan" is defined as moving the beam position at the target without changing the angle. "Angle scan" means changing the beam angle without changing the beam position. The numbers were calculated for a beam energy of 800 Gev.

Table 2.6.1  
Target Scan Capabilities

Type of Scan	Horizontal	Vertical
Position	7 mm	5 mm
Angle	200 $\mu$ rad	1.8 mrad

Target scan capabilities with proposed beamline. Calculations are based on 800 GeV.

These numbers are calculated using the relation between magnet fields and SWICs positions given in section 2.5. For example, for a horizontal position scan the matrix relation plus the constraint that the beam moves the same amount in NM2WC2 and NM2WC3 were used.

## 2.7 Instrumentation

### 2.7.1 NM1

Two short external beam BPMs and a vacuum SWIC in NM1 are needed. This instrumentation is used on a regular basis at the Lab.

## 2.7.2 NM2

Two short BPMs and a vacuum SWIC for the upstream end of NM2 are needed. Again this is instrumentation used on a regular basis at Fermi Lab. For the region near the target, very good position resolution and the ability to accurately measure beam profiles is also needed. The current plan is to develop a wire SEM with 100 micron wire spacing. The standard wire SEMs that have been used in the past at the Lab do not work with slow spill. The reason for this is that the signal is too small when spread over 20 seconds. To enhance the signal the wires can be coated with CsI. These CsI coated wire SEMs have been tried at CERN and proved to work. The plan to acquire the expertise at the Lab is the following: a) the EED department is building a 100 micron wire spacing SEM, b) the CsI coating of the wires is going to be done by Dave Anderson's PDG Group, and c) the wire SEM is going to be tested at BNL.

How well can the average beam position with a 100 micron wire spacing instrument be measured? If the channels of the Scanner are all equal and the beam spans several wires, the average can be measured at least an order of magnitude better than the wire spacing. Of course there are problems with the Scanner, halo, etc. Figure 2.7.1 is a practical case of a one millimeter SWIC used with a regular Scanner. Each point in the figure corresponds to the average of the SWIC profile in the middle of the spill. A change of 150 parts per million in the beam momentum or in the NE9E currents produced a one millimeter displacement in the beam position (y axis in the figure) at NECPWC<sup>19</sup>. So the beam position oscillation seen in the figure represents an instability of 150 ppm peak to peak. The data was taken at the end of the last Fixed Target run and there was no time to determine if the oscillation was caused by changes in the momentum or the NE9E magnets. However, it can be seen that the beam average was measured to better than one fifth of a wire spacing. This claim can be made because the difference between two successive points is on the average better than one division. The assumption is that with the 100 microns wire spacing SEM, one can determine the average beam position to 20 microns.

---

<sup>19</sup> NE9E is a string of five B1 magnets.

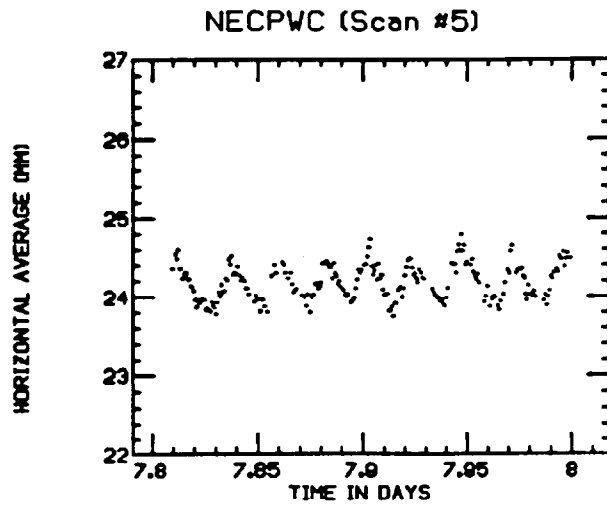


Figure 2.7.1

Average beam position at NECPWC as a function of time. Each point corresponds to a SWIC reading in the middle of the spill. The units are millimeters and days. The oscillation is due to a change of 150 ppm in either the beam momentum or the NE9E current.

## 2.8 Muon Halo

This section will concern itself with muons transported to the target along with the primary beam. These muons will be assumed to have been produced from interactions at four different points: MuSep, MuBend, H424, and NM1. In all models a primary beam energy of 800 GeV and a 20s spill time is assumed. In this section, the detector is assumed to be a 4m by 4m area centered on the neutral beam, located 185m downstream of the target.

### 2.8.1 HALO Calculations and Impact

The program HALO was used to simulate beam interaction and muon production. Figure 2.8.1. shows the elements used in the model, with production points indicated by an asterisk. A primary beam intensity of  $5 \times 10^{12}$  ppp was assumed. HALO assumes muon production from four sources:  $\pi^+$ ,  $\pi^-$ ,  $K^+$ , and  $K^-$  decay. A separate run must be made for each production source. In all models, production is assumed to occur from one million protons interacting with one radiation length of iron. After each run, the muon distribution at the target was written to a file. This file was then used as the input spectrum to TRAMU, which transported the muons to the detector.<sup>20</sup>

---

<sup>20</sup> TRAMU is a subroutine in CASIMU which is responsible for muon transport. CASIMU will be detailed more fully in Section 4.4.2.

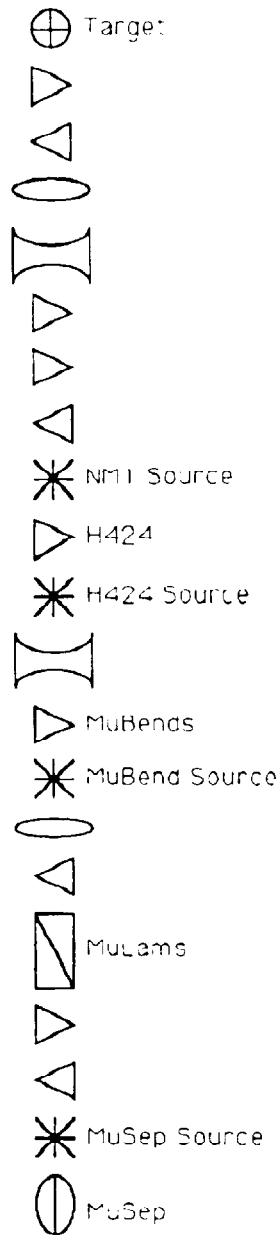


Figure 2.8.1  
 Primary Beam Layout Used to Model Muon Halo  
 (Schematic - not to scale)

Table 2.8.2 shows the resulting muon rates at the target hall and the detector plane. Results are summarized in muons per interacting proton (p\*) and kHz per interaction proton.

Table 2.8.2  
Summary of Muon Halo

Location	Target Hall		Detector Plane	
	muon/p*	kHz/p*	muon/p*	kHz/p*
MuSep	2.18E-04	1.09E-08	0.00E00	0.00E00
MuBend	6.48E-05	3.24E-07	7.89E-07	3.95E-11
H424	4.29E-03	2.14E-07	2.67E-04	1.34E-08
NM1	6.42E-04	3.21E-08	2.80E-05	1.04E-09

Muon halo per interacting proton (p\*) tabulated for various sources.

H424 is the worst source for halo, due to the long (~800 foot) straight section between it and the next bend (located in NM1). This allows plenty of space for pions produced at H424 to decay.

Table 2.8.3 summarizes potential interactions and resulting rates at the detector.

Table 2.8.3  
Background at Detector

Location	Source	Rate
H424	3mil Ti vacuum window	19 kHz
NM1	Vacuum SWIC	16 kHz
TOTAL:		35 kHz

Projected halo background at the detector for  $5 \times 10^{12}$  protons.

Table 2.8.4 summarizes rates at the detector due to 1% beam scraping at four locations.

Table 2.8.4  
Rates Due to 1% Beam Scraping

Location	Rate
MuSep	0 kHz
MuBend	2.0 kHz
H424	670 kHz
NM1	35 kHz

### 2.8.2 Operational Expectations, Control

Clearly, beam scraping must be avoided and as little instrumentation as possible must remain in the beam.

The SWIC in NM1 may be kept out of the beam, except for diagnostic use. As the window at H424 separates the cryogenic vacuum system from the conventional vacuum system, this source cannot be eliminated.

Adequate control must be provided in order to reduce beam scraping to less than 0.01% at H424 and 0.1% at NM1. This would result in background due to beam scraping at the 10kHz level.

## 2.9 Component Identification

All the magnets exist. Four beam line BPMs and their associated electronics have to be acquired. The two target wire SEMs and the associated scanner have to be developed. The two vacuum SWICs and the intensity monitor SEM already exist.

### 2.10 RD/AD Beam Control Link

The plan is to use ACNET (the Accelerator Division Beam Control System) to correct for beam roll. To correct for instabilities that happen over a time scale of a few spills or more, the plan is to use EPICURE (Research Division Beam Control System). Therefore a communication channel

between the two systems is needed. The ACNET system needs to be able to read the BPMs and the SWICs in NM2, and the EPICURE system needs to be able to read the current changes in the part of the KTeV beam line that is controlled by ACNET.

## 3. CRITICAL DEVICES / INTERLOCKS

### 3.1 Primary Beam

#### 3.1.1 Precluding Downstream Primary Transport

A combination of careful alignment, configuration control processes, and active current interlocks will be used to prevent the primary beam at 800 GeV from exiting the KTeV Target Pile:

1. Interlock the AVB currents to  $I_{NM2D1} + 0.5 \cdot I_{NM2D2} \geq 4630$  amps. This will ensure that the minimum targeting angle will be  $-4.0$  mrad. These supplies should also be controlled such that they will always bend positively charged particles down.
2. Interlock the NM2EU current to  $\pm 68$  amps from the nominal value.
3. NM1U and NM2EU will be used as collimators to limit positions excursions. Therefore they must be carefully aligned and their configuration maintained by using "RED TAGS" on lock outs on position-adjusting devices.
4. Interlock the quadrupole currents to:

$$0.217 I_{NM2Q1} + I_{NM2Q2} = -567 \pm 86 \text{ amps}$$

and

$$I_{NM2Q1} \leq 1011 \text{ amps}$$

The extreme position changes allowed with these interlocks are shown on Figure 3.1.1, which is taken directly from Appendix 2. The precise values of the current interlocks depend on the final configuration of the Primary Beam line, but the methodology presented in Appendix 2 is applicable in case this should change.

Primary beam must not be transported through the neutral beam channel into the KTeV experimental hall since it is designed only to accept secondary beam of much lower energy and intensity. In addition beam line elements downstream of the targeting station within NM2 are not set to transport 800 GeV particles. Because of this, the introduction of primary beam into the neutral beam channel could result in higher than normal

losses downstream of the targeting station. This could cause significant residual radiation dose rates, contamination, and increased air activation. Routine maintenance and unscheduled repairs would be more difficult. Therefore the goal in selecting the interlocks is to insure that the 800 GeV primary beam is confined to the well-shielded target station.

To prevent the beam from exiting the KTeV Target Pile, we specifically prevent an 800 GeV primary proton from entering the neutral beam aperture of NM2S2, the first major element downstream of the KTeV Target Pile. The calculations for these interlocks were done to prevent a primary proton having the maximum possible deviation from the beam centerline from leaving NM2BD (the NM2 Beam Dump). The maximum allowed deviation from the primary beam centerline places a primary proton on the edge of the aperture of the Beam Dump. The assumptions to insure careful alignment between NM1 and NM2 are that when the beam is vertically centered at NM1U and NM2EU, the quadrupoles do not significantly steer the beam and the incoming angle of the beam on the target is minimally -4.00 mrad. These assumptions are easily checked when the beam is first turned on. The NM2S1 magnet (the Target Sweeping Magnet) running at the nominal 5kG will not provide adequate protection to prevent beam from being horizontally steered into the neutral channel of the secondary beam, so all calculations were applied to achieve adequate protection through vertical steering. The resulting current limits on the NM2 magnets were based on limiting the possible angles that a primary beam can have going into the quadrupoles. The interlock on NM2S2 was calculated to prevent beam from being directed into NM3 in the accident case of the AVB system tripping off.

Please see Appendix 2 for a detailed discussion on the calculation of these interlocks.

KTeV Primary Beamline Apertures - NM1 through NM2  
Elevation view

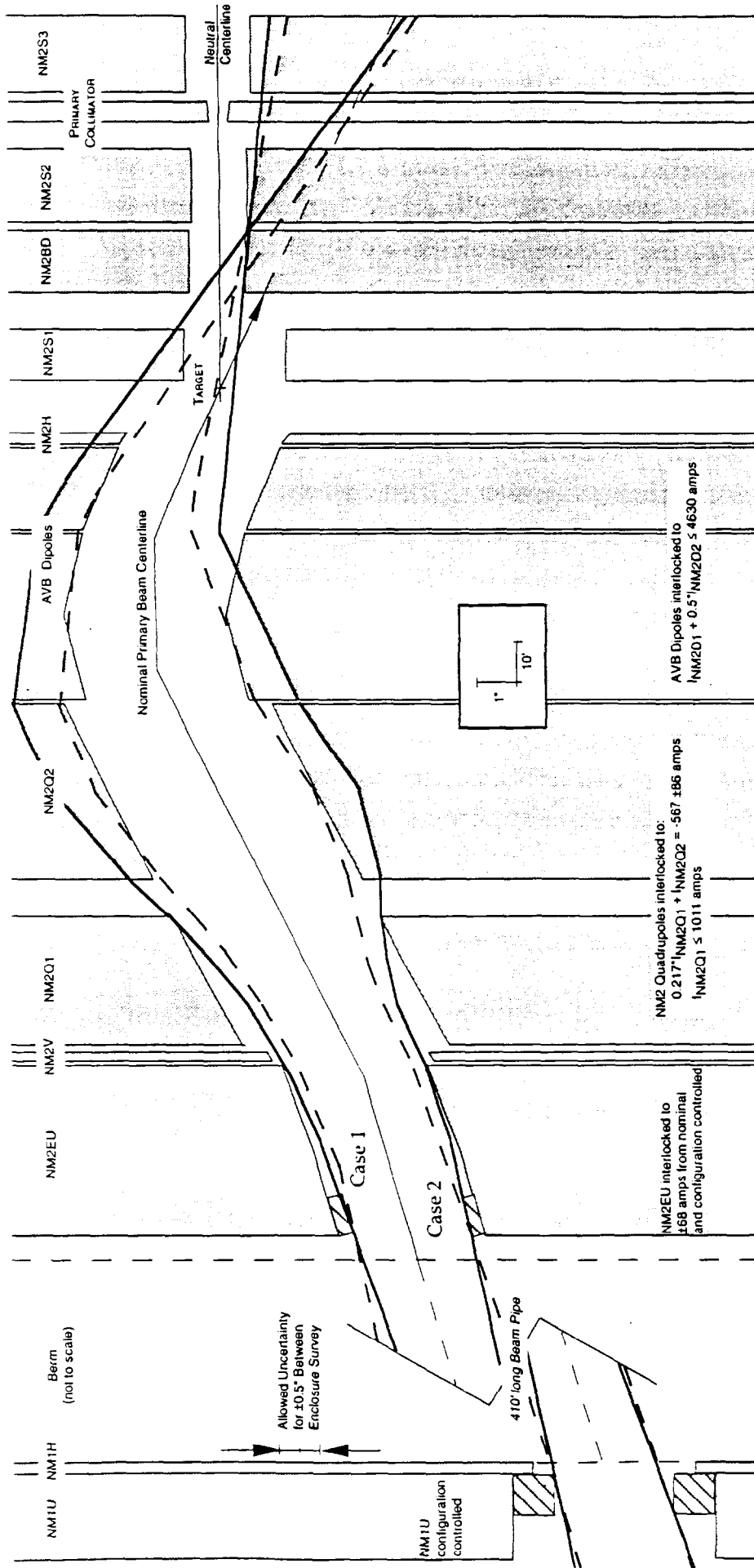


Figure 3.1.1: KTeV Primary Apertures. Shown here are the vertical apertures for the magnets from NM1 to the KTeV Target Hall, with the Nominal Primary Beam Centerline shown for the path of primary beam with the AVB system set to bend the beam to  $-4.00$  mrad at the Target. The two extremes shown as thick solid lines are for beam entering NM2 at  $\pm 0.6629$  mrad relative to the nominal beam trajectory, the beam paths from the lower aperture limit of either NM1U or NM2EU to the upper aperture limit of the other. The thick dashed lines are for beam entering at  $\pm 0.0947$  mrad relative to the nominal beam trajectory, the beam path due to the allowed survey tolerance between enclosures, staying on the same side of the nominal beam along the edge of the NM1U and NM2EU apertures. The solid beam paths cross each other in the beam pipe region between NM1 and NM2. The magnets are set to produce the maximum allowed deviation from the nominal with these extremes at the downstream end of the Beam Dump.

Case 1 is for the NM2 quadrupoles set to  $R_{21} = -0.500$  mrad/cm and  $R_{43} = -0.430$  mrad/cm.

Case 2 is for the NM2 quadrupoles set to  $R_{21} = -0.500$  mrad/cm and  $R_{43} = -0.687$  mrad/cm.

For both cases, the AVB system is set to its minimum limit, and NM2EU & NM2V to their maximum upward bending limits. The range for allowable quadrupole current settings lie between these extremes. Note that the AVB and NM2S1 magnets are not configuration controlled in this scheme. [From Figure A3.1 from Appendix 3.]

### 3.1.2 Critical Devices/Coupling with Neutrino Area

Besides the special interlocks listed in Section 3.1.1 to preclude primary beam transport downstream of the target hall, the KTeV primary beam will utilize upstream Critical Devices, that when disabled will protect the KTeV beam enclosures and experimental area from any beam transport, and hence any significant prompt radiation.

The primary beam Critical Devices for KTeV are the same as used in previous runs for the NMUON beam line. These are MULAM and MUBD located in the AD Switchyard beam transport system. These elements will continue to have typical Research Division Critical Device interlocks fitted, as well as a Failure Mode Backup circuit, which reverts to disabling upstream Switchyard devices to ensure further redundancy in safety protection.

All enclosures associated with the KTeV beamline will have standard Research Division enclosure interlocks which will monitor all access points. Each Interlock Section will have a Radiation Detector Chassis incorporated into the Summation Chassis to permit the use of interlocked detectors if the need arises.

Monitoring of target hall magnet temperatures and flow of RAW cooling water can also be sensed by the interlock system.

As for previous running of the NMUON beamline, shared tunnel geometry imposes a strong coupling between KTeV beam operation and interlock status of the Neutrino Area upstream enclosures. The Neutrino Primary run condition must be satisfied to operate KTeV beam.

## 3.2 Secondary Beam

### 3.2.1 Critical Devices

A required feature, due to the location of the KTeV experimental area in the upstream NMUON beam area, is that disabling of the primary beam to NM2 will be needed to ensure radiation protection for the NM3 secondary beam enclosure and the KTeV experimental hall.

This is due to the intense muon fluxes present in these enclosures from primary beam dumping in the NM2 target hall. Projected muon rates in the decay enclosure and experimental hall are shown in Figures 4.4.10 and 4.4.11. These rates could be reduced somewhat by requiring the primary target to move to an "out" position as part of disabling the secondary beam. However, even then they would still be well above the 2.5 mr/hr limit for access into the enclosures.<sup>21</sup>

Hence, the same critical devices MULAM and MUBD are projected for the KTeV secondary beam. A fast activated beam stop is planned to be installed in NM2 downstream of the beam dump system, which will selectively stop the neutral hadron beam from exiting NM2. The function of this device is very useful for aiding in selective radiation and particle rate measurements in the downstream enclosures. However, it is not adequate as a Critical Device element due to the beam dump muon fluxes.

### 3.2.2 Experimental Hall Interlocks

The decay enclosure and the experimental hall will also have standard Research Division enclosure interlocks and a Radiation Detector Chassis incorporated into the Summation Chassis in order to monitor and/or control prompt radiation rates.

---

<sup>21</sup> W. S. Freeman, et al., "Radiation Shielding Requirements for the KTeV Facility," January 13, 1993.

Access interlock doors between the counting room area and the experimental hall will be positioned in the passage ways to the experimental hall, allowing unlimited access in the counting room areas outside of these doors. The results of calculations addressing radiation levels in these passages are presented in Section 6.

### **3.3 Access Issues**

#### **3.3.1 Access Requirements**

The capability to separately and efficiently access each Fixed Target experimental hall with minimal impact to other experiments has been very important for the operational efficiency of the external areas Fixed Target program. The detector system redundancies built of necessity into the large collider detectors, due to their limited access options, are extremely expensive and not a realistic option for the Fixed target detectors.

Timely access into the experimental hall is especially important for the KTeV experiments due to the precision measurements involved. This has been reaffirmed in the Oct.'93 Director's Review of KTeV, and was recommended by that Review Committee as an Action Item to be accomplished for KTeV.

#### **3.3.2 Options Considered**

There are three currently accepted methods of controlling Fixed Target experimental hall radiation levels during access conditions. Each has been evaluated for possible KTeV application.

The first method is to utilize enough shielding between the targeting enclosure and the experimental hall to sufficiently range out the bulk of muons produced in the target pile. This method, suitable for long secondary beam lines, allows access into the experimental hall with the least disruption in overall program stability. By use of standard Research Division Access Device Controllers the secondary beam created from normal targeting is blocked with the use of redundant beam stops located downstream of the

target pile. This approach can be used when a prompt dose rate less than 2.5 mr/hr can be maintained during the access with continued primary beam targeting. As indicated in Section 3.2, beam dump muon fluxes preclude this method for KTeV with its short secondary beam length.

A second method is to utilize a separate RAW cooled dump system at a location upstream of the targeting enclosure. Size of the dump and its cost is driven by the intensity and duration projected for dumping the beam. Two factors which must be considered are groundwater activation and radiation rates, both prompt and residual. This was the method available in previous running in the Meson Area, where the pre-Tev II target piles remained available for use during either current targeting enclosure or experimental hall accesses.

For KTeV, the installation of an upstream RAW cooled beam dump could possibly be located in the downstream end of the AD/Switchyard Enclosure G2, if this were the method chosen. Other location options between G2 and NM1 would require new civil construction.

The third access method is to take away the KTeV primary beam using the upstream electrostatic septa splitting station, and redistribute it as feasible to other beamlines. Historically, this is the least preferable method due to the considerable disruption to other beam users. If this were the method chosen for KTeV, practical application difficulties should make as a priority task an effort to automate and improve the efficiency with which the various Switchyard primary beam intensities can be controlled. Significant prototyping efforts including beam tests have previously taken place toward this end, as there would be significant improvement in operational efficiency for all fixed target users. The location of the Switch Yard electrostatic septa splitting station for KTeV, downstream of other area septa splits, also makes this a more challenging task to accomplish quickly for this beam without beam splitting control upgrades. This is due to beam tails from other splits effectively expanding the size of the beam to KTeV.

Resolution of a practical and reasonable access method to the KTeV experimental hall remains a major unresolved issue, needing approval and effort from both the lab Research and Accelerator Divisions.